

Rigidification of a Macroyclic *Tris*-Catecholate Scaffold Leads to Electronic Localisation of its Mixed Valence Redox Product

Sam Greatorex^a, Kevin B. Vincent^b, Amgalanbaatar Baldansuren^c, Eric J. L. McInnes^c, Nathan J. Patmore^b, Stephen Sproules^d and Malcolm A. Halcrow^{a,*}

^aSchool of Chemistry, University of Leeds, Woodhouse Lane, Leeds LS2 9JT,
United Kingdom.
E-mail: m.a.halcrow@leeds.ac.uk

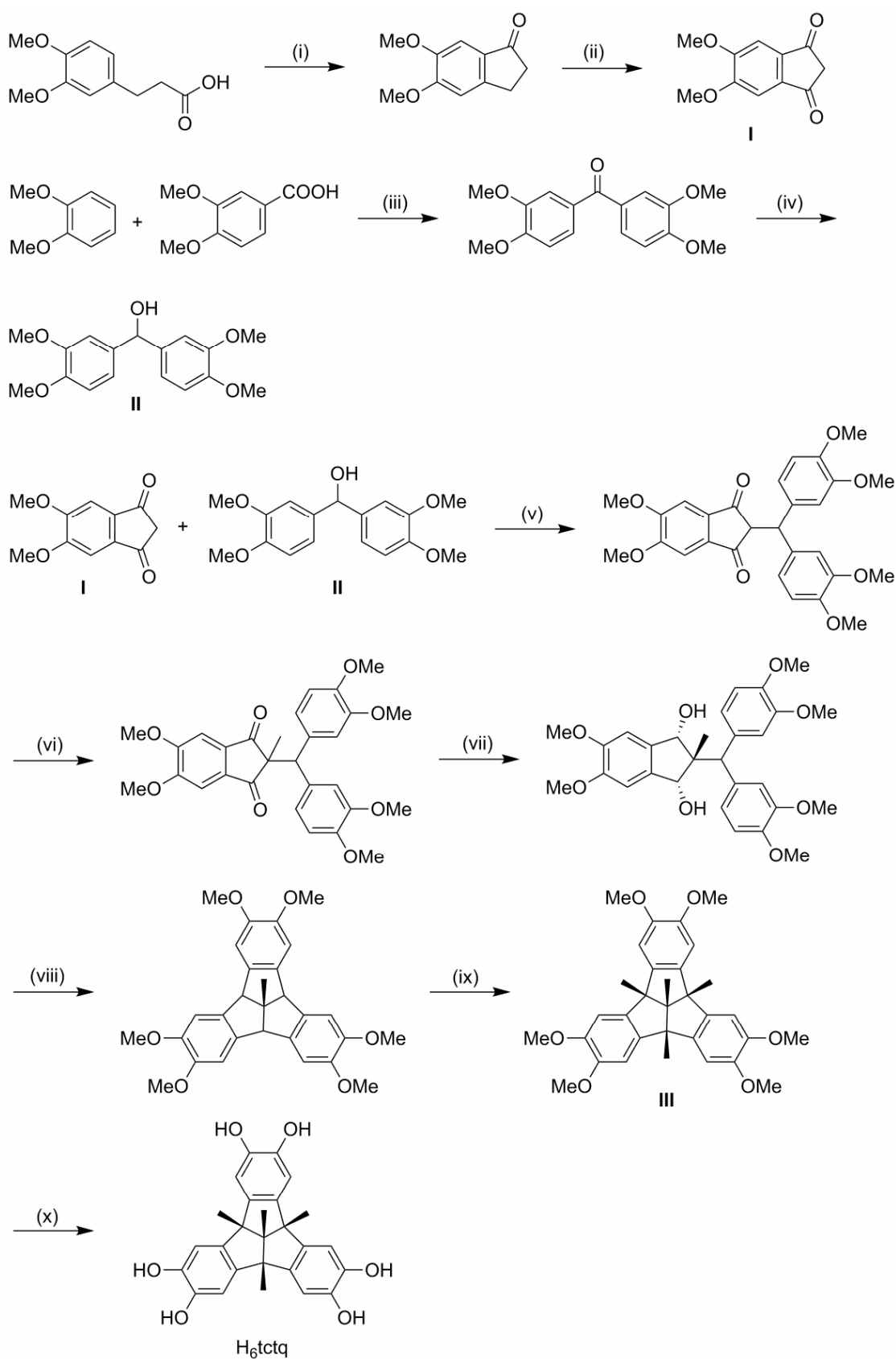
^bDepartment of Chemical Sciences, University of Huddersfield,
Huddersfield HD1 3DH, UK.

^cSchool of Chemistry and Photon Science Institute, University of Manchester,
Oxford Road, Manchester M13 9PL, UK.

^dWestCHEM, School of Chemistry, University of Glasgow, Glasgow G12 8QQ, UK.

Supporting Information

	Page
Scheme S1 Synthesis of H ₆ tctq.	2
Experimental Details	3
Table S1 Crystallographic experimental data for H ₆ tctq·thf·nMeOH.	4
Figure S1 ¹ H NMR spectrum of H ₆ tctq.	5
Figure S2 View of the H ₆ tctq·thf moiety in the structure of H ₆ tctq·thf·nMeOH.	6
Table S2 Hydrogen bond parameters in the structure of H ₆ tctq·thf·nMeOH.	6
Figure S3 The hydrogen bond connectivity in H ₆ tctq·thf·nMeOH	7
Figure S4 A hydrogen bonded bilayer in the lattice of H ₆ tctq·thf·nMeOH.	8
Figure S5 The inclusion of thf molecules inside the H ₆ tctq bowl-shaped cavities in H ₆ tctq·thf·nMeOH.	9
Figure S6 Overlays of the crystallographic molecular structures of H ₆ tctq and H ₆ ctc, showing the shallower bowl-shaped conformation of the H ₆ tctq macrocycle.	9
Figure S7 High-resolution electrospray mass spectrum of 2a .	10
Figure S8 The 2a →[2a ·] ⁺ oxidation monitored by titration with [FeCp ₂]PF ₆ by UV/vis/NIR spectroscopy.	11
Figure S9 Measured and simulated X-band EPR spectrum of [2a ·] ⁺ in CH ₂ Cl ₂ solution at 150 K.	12
Figure S10 Measured and simulated S-band EPR spectra of [2a ·] ⁺ in CH ₂ Cl ₂ solution at 300 K and 45 K.	12
Figure S11 Measured and simulated EPR spectra of [2b ·] ⁺ in CH ₂ Cl ₂ solution.	13
Table S3 Simulated EPR parameters for [2a ·] ⁺ and [2b ·] ⁺ in CH ₂ Cl ₂ solution.	13
Table S4 Calculated mean bond distances and angles in the different oxidation states of 2a .	14
Table S5 Geometry optimized coordinates for 2a .	15
Figure S12 MO energy level scheme of frontier Kohn-Sham orbitals for 2a with C _{3v} symmetry labels.	17
Table S6 Geometry optimized coordinates for [2a ·] ⁺ .	18
Figure S13 MO energy level scheme of frontier Kohn-Sham orbitals for [2a ·] ⁺ .	20
Table S7 Geometry optimized coordinates for [2a ···] ²⁺ .	21
Figure S14 MO energy level scheme of frontier Kohn-Sham orbitals for [2a ···] ²⁺ .	23
Table S8 Geometry optimized coordinates for [2a ···] ³⁺ .	24
Figure S15 MO energy level scheme of frontier Kohn-Sham orbitals for [2a ···] ³⁺ .	26
Figure S16 Mulliken spin population analyses for [2a ·] ⁺ , [2a ···] ⁺ and [2a ···] ³⁺	27
References	28



Scheme S1. Synthesis of H_6tctq . Steps (i)-(ix) are taken from ref. 1. Reagents and conditions: (i) $(\text{COCl})_2$, dmf , CH_2Cl_2 , rt, 18 hrs then AlCl_3 , CH_2Cl_2 , rt, 2 hrs, 34 %; (ii) CrO_3 , $\text{AcOH}/\text{H}_2\text{O}$, $0^\circ\text{C} \rightarrow \text{rt}$, 3 days, 19 %; (iii) Polyphosphoric acid, 80°C , 30 min then ice, 75 %; (iv) 10 bar H_2 , Pd/C , pyridine, MeOH , rt, 4 days, 70 %; (v) TsOH , toluene/ CH_2Cl_2 , reflux, 18 hrs, 89 %; (vi) MeI , KF/celite , MeCN , reflux, 18 hrs, 74 %; (vii) DIBAL , toluene, $0^\circ\text{C} \rightarrow \text{rt}$, 18 hrs, 81 %; (viii) H_3PO_4 , chlorobenzene, reflux, 1 hr, 36 %; (ix) NBS/AIBN , benzene, $h\nu$, 45 mins then AlMe_3 , toluene, 50°C , 1 hr, 25 %; (x) BBr_3 , CH_2Cl_2 , 0°C , 6 hrs, 98 %.

Experimental

2,3,6,7,10,11-Hexamethoxy-4b,8b,12b,12d-tetramethyltribenzotriquinacene (compound **III**, Scheme S1)¹ and $[\text{PtCl}_2\text{L}]$ ($\text{L} = \text{dppb}$, dppe)² were prepared by the literature procedures. Other reagents and solvents were purchased commercially and used as supplied.

Synthesis of 2,3,6,7,10,11-hexamethoxy-4b,8b,12b,12d-tetramethyltribenzotriquinacene (H₆tctq). To a stirred solution of 2,3,6,7,10,11-hexamethoxy-4b,8b,12b,12d-tetramethyltribenzotriquinacene (0.12 g, 0.23 mmol) in dry dichloromethane (6.5 cm³) in an ice bath under N₂ was added boron tribromide (0.38 g, 1.52 mmol). After stirring for 6 hrs the mixture was poured onto ice (40 g) and stirred at room temperature until the ice melted. The resultant pale red precipitate was collected by filtration, washed with water (3 x 5 cm³) and dried *in vacuo*. Yield 0.094 g, 98 %. Mp 350 °C dec. ¹H NMR ($\{\text{CD}_3\}_2\text{CO}$) δ 1.23 (s, 3H, CH₃), 1.34 (s, 9H, CH₃), 6.63 (s, 6H, CH), 7.37 (br s, 6H, OH). HR-ESMS *m/z*: 453.1265 (calcd for [C₂₆H₂₂O₆Na]⁺ 453.1309).

Synthesis of $[\{\text{Pt}(\text{dppb})\}_3(\mu_3\text{-tctq})]$ (2a). A mixture of H₆tctq (0.018 g, 0.043 mmol) and $[\text{PtCl}_2(\text{dppb})]$ (0.10 g, 0.14 mmol) in dry deoxygenated *N,N*-dimethylacetamide (10 cm³) was stirred for 30 mins under a nitrogen atmosphere, before potassium *tert*-butoxide (0.040 g, 0.36 mmol) in dry deoxygenated methanol (5 cm³) was added dropwise. The mixture turned from yellow to green and was stirred for 18 hours. Dry deoxygenated diethyl ether (20 cm³) was added, and the mixture was cooled in an ice bath for 30 minutes before being filtered by cannula to afford a pale green powder. The product was recrystallised from a chloroform/pentane solvent mixture. Yield 0.064 g, 63 %. Found C, 49.0; H, 3.47; N, 0.00 %. Calculated for C₁₁₆H₉₀O₆Pt₃·4CHCl₃ C, 49.3; H, 3.25; N, 0.00 %. ESMS *m/z*: 685.1 ($[\{\text{Pt}(\text{dppb})(\text{O}_2\text{CH})-\text{H}\}]^+$), 856.2 ($[\{\{\text{Pt}(\text{dppb})\}_2(\text{H}_2\text{tctq})+2\text{H}\}]^{2+}$), 1175.2 ($[\{\{\text{Pt}(\text{dppb})\}_3(\text{tctq})+\text{H}\}]^{2+}$), 1398.1 ($[\{\{\text{Pt}(\text{dppb})\}_3(\text{dppb})(\text{tctq})+\text{H}\}]^{2+}$), 1711.3 ($[\{\{\text{Pt}(\text{dppb})\}_2(\text{H}_2\text{tctq})+\text{H}\}]^+$), 2350.4 (calcd for $[\{\{\text{Pt}(\text{dppb})\}_3(\text{tctq})+\text{H}\}]^+$). ¹H NMR (CD_2Cl_2) δ 1.12 (s, 3H, tctq CH₃), 1.36 (s, 9H, tctq CH₃), 6.47 (s, 6H, tctq CH), 7.40-7.85 (m, 72H, dppb CH). ³¹P{¹H} NMR (CD_2Cl_2) δ 29.9 ($J_{\text{P}-195\text{Pt}} = 3358$ Hz).

Synthesis of $[\{\text{Pt}(\text{dppe})\}_3(\mu_3\text{-tctq})]$ (2b). Method as for **2a**, using $[\text{PtCl}_2(\text{dppe})]$ (0.093 g, 0.14 mmol). The product was isolated as a sparingly soluble pale green powder, of which small amounts could be purified by recrystallisation from chloroform/pentane. Yield 0.047 g, 50 %. Found C, 48.4; H, 3.15; N, 0.00 %. Calculated for C₁₀₄H₉₀O₆Pt₃·4CHCl₃ C, 48.3; H, 3.52; N, 0.00 %. ESMS (dmso) *m/z*: 636.1 ($[\{\text{Pt}(\text{dppe})(\text{O}_2\text{CH})]\}^+$), 670.1 ($[\{\text{Pt}(\text{dppe})(\text{dmso})]\}^+$), 1693.2 ($[\{\{\text{Pt}(\text{dppe})\}_2(\text{H}_2\text{tctq})(\text{dmso})+\text{H}\}]^+$).

The compound was insufficiently soluble to afford useful NMR spectra.

Single crystal X-ray structure determination of H₆tctq·thf·nMeOH

The crystals were obtained by storage of a solution of H₆tctq in a thf/methanol mixture, at -15 °C. Diffraction data were collected with an Agilent Supernova diffractometer, using monochromated Cu-*K*_α radiation ($\lambda = 1.54184$ Å). The diffractometer is fitted with an Oxford Cryosystems low-temperature device. Experimental details of the structure determination are given in Table S1. The structure was solved by direct methods (*SHELXS97*³), and developed by least-squares refinement on F^2 (*SHELXL97*³). Crystallographic figures were prepared using *X-SEED*.⁴

The asymmetric unit contains one molecule of interest, and one fully occupied molecule of thf. Two weak residual Fourier peaks near the crystallographic inversion centre $\frac{1}{2}$, $\frac{1}{2}$, 0 were also included in the model as a 0.15-occupied molecule of methanol. All fully occupied non-H atoms were refined anisotropically. The tctq O-bound hydroxyl H atoms were located in the Fourier map and were allowed to refine, with U_{iso} restrained to 1.5x U_{eq} of the corresponding O atom. Other H atoms were placed in calculated positions and refined using a riding model. An antibumping restraint was applied to the fractional methanol OH group, to ensure a reasonable geometry.

Table S1 Crystallographic experimental data for H₆tctq·thf·nMeOH ($n \approx 0.15$).

Molecular formula	C _{30.75} H _{33.80} O ₇	V / Å ³	1273.1(3)
M_r	515.38	Z	2
Crystal system	triclinic	$\mu\{\text{Cu}-K_{\alpha}\} / \text{mm}^{-1}$	0.772
Space group	$P\bar{1}$	T / K	120(2)
<i>a</i> / Å	11.1115(13)	Measured reflections	9545
<i>b</i> / Å	11.3585(16)	Independent reflections	4773
<i>c</i> / Å	12.7308(15)	R_{int}	0.060
α / °	67.602(12)	$R_1, I > 2\sigma(I)^a$	0.082
β / °	67.891(11)	wR_2 , all data ^b	0.247
γ / °	62.042(13)		

^a $R = \sqrt{\frac{\sum |F_o| - |F_c|}{\sum |F_o|}}$ ^b $wR = [\sum w(F_o^2 - F_c^2) / \sum wF_o^4]^{1/2}$

Other measurements

Elemental microanalyses were performed by the London Metropolitan University microanalytical service. Electrospray mass spectra (MS) were obtained on a Bruker MicroTOF spectrometer, from MeCN feed solutions. All mass peaks have the correct isotopic distributions for the proposed assignments. Alkali metal cations and formate anions in the molecular ion assignments originate from calibrants in the spectrometer feed solutions. NMR spectra were run using a Bruker Avance 500 spectrometer operating at 500.1 MHz (¹H) or 125.6 MHz (³¹P). UV-vis/NIR spectra for redox titrations were run on a Perkin Elmer Lambda900 spectrophotometer using 1 cm quartz cells.

Electrochemical measurements were carried out using an Autolab PGSTAT204 voltammetric analyser, under an argon atmosphere, in predried CH₂Cl₂ containing 0.1 M ⁷Bu₄NPF₆ as supporting electrolyte. Voltammetry experiments used a Pt disk working electrode, a Pt rod counter electrode and an Ag/AgCl reference electrode. All potentials quoted are referenced to internal ferrocene and were obtained at a scan rate (*v*) of 100 mV s⁻¹. The Fc⁺⁰ couple under these conditions was observed at $E_{1/2} = +0.48 \pm 0.01$ V vs. Ag/AgCl. UV-vis/NIR spectroelectrochemistry experiments were conducted using a Shimadzu UV-3600 plus spectrophotometer, fitted with an optically transparent thin layer electrode (OTTLE) cell. The working electrode was platinum gauze in the path of the beam, the counter electrode was platinum wire, and silver wire was used as the reference electrode. The electrolysis was controlled by an Autolab PGSTAT 100N.

Multifrequency EPR measurements were carried out at the EPSRC National UK EPR Facility and Service in the Photon Science Institute at The University of Manchester. Samples were prepared by oxidation of the neutral complex by ferrocenium hexafluorophosphate in CH₂Cl₂ solution at -78 °C with a concentration of 3-5 mM. A small amount of THF was added to the reaction mixture before samples were loaded into the appropriately sized quartz tubes. S-band (*v* = 3.86 GHz) and X-band (*v* = 9.41 GHz) continuous wave spectra were collected using a Bruker EMX spectrometer. Spectrum simulations were performed using *Easyspin*.⁵

Calculations

The ORCA program package was used for all calculations.⁶ The geometries of all molecules were fully optimised by a spin-unrestricted DFT method employing the BP86 functional⁷ and the D3 dispersion correction.⁸ Starting coordinates were adapted from the crystallographic coordinates of **1a**⁹ with the Ph rings of dppb replaced with H atoms. Split-valence basis sets with one set of polarisation functions (def2-SVP) were used for all atoms.¹⁰ Auxiliary basis sets used to expand the electron density in the calculations were chosen to match the orbital basis. The self-consistent field calculations were tightly converged ($1 \times 10^{-8} E_h$ in energy, $1 \times 10^{-7} E_h$ in the charge density, and 1×10^{-7} in the maximum element of the DIIS¹¹ error vector). The geometry was converged with the following convergence criteria: change in energy $< 10^{-5} E_h$, average force $< 5 \times 10^{-4} E_h \text{ Bohr}^{-1}$, and the maximum force $10^{-4} E_h \text{ Bohr}^{-1}$. The geometry search for all complexes was carried out in redundant internal coordinates without imposing geometry constraints.

Electronic properties were calculated on the optimised coordinates at the B3LYP level of theory.¹² Calculations with this hybrid functional used the RIJCOSX algorithm to speed the calculation of Hartree–Fock exchange.¹³ A segmented all-electron relativistically contracted SARC-ZORA-TZVP basis set was used for platinum with increased integration accuracy (SPECIALGRIDINTACC 10).¹⁴ The scalar relativistically recontracted ZORA-def2-

TZVP basis set was used for all other atoms.¹⁵ Calculations included the zeroth-order regular approximation (ZORA) for relativistic effects¹⁶ as implemented by van Wüllen.¹⁷ The conductor-like polarizable continuum model (CPCM) was employed using an infinite continuum.¹⁸

We used the broken symmetry (BS) approach to describe our computational results for $[2\bullet]^{2+}$ and $[2\bullet\bullet]^{3+}$.¹⁹ We adopt the following notation: the given system was divided into two fragments. The notation BS(m, n) refers then to a broken symmetry state with m unpaired α -spin electrons essentially on fragment 1 and n unpaired β -spin electrons localized on fragment 2. In most cases, fragments 1 and 2 correspond to the metal and the ligands, respectively. In this notation the standard high-spin, open-shell solution is written as BS($m+n, 0$). The BS(m, n) notation refers to the initial guess to the wave function. The variational process does, however, have the freedom to converge to a solution of the form BS($m-n, 0$) in which effectively the $n\beta$ -spin electrons pair up with $n < m$ α -spin electrons on the partner fragment. Such a solution is then a standard $M_s \equiv (m-n)/2$ spin-unrestricted Kohn-Sham solution. As explained elsewhere,²⁰ the nature of the solution is investigated from the corresponding orbital transformation (COT) which, from the corresponding orbital overlaps, displays whether the system should be described as a spin-coupled or a closed-shell solution. Corresponding¹⁶ and canonical orbitals and density plots were obtained using Molekel.²¹

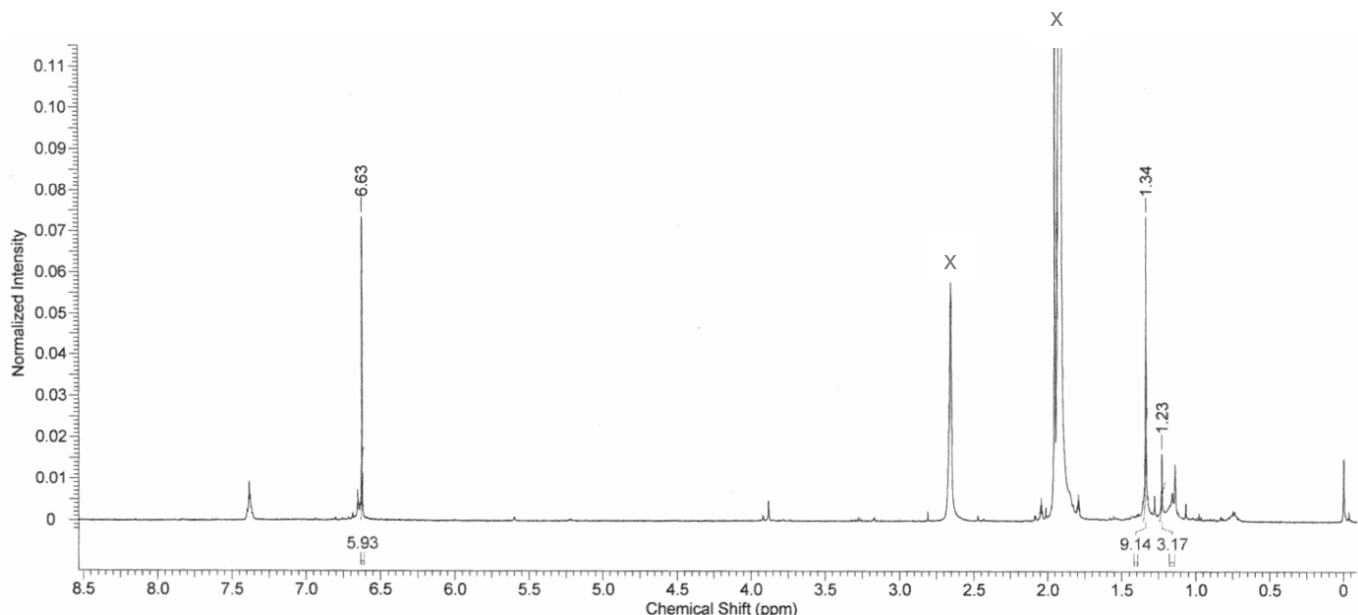


Figure S1. ^1H NMR spectrum of $\text{H}_6\text{tctq} (\{\text{CD}_3\}_2\text{CO})$.

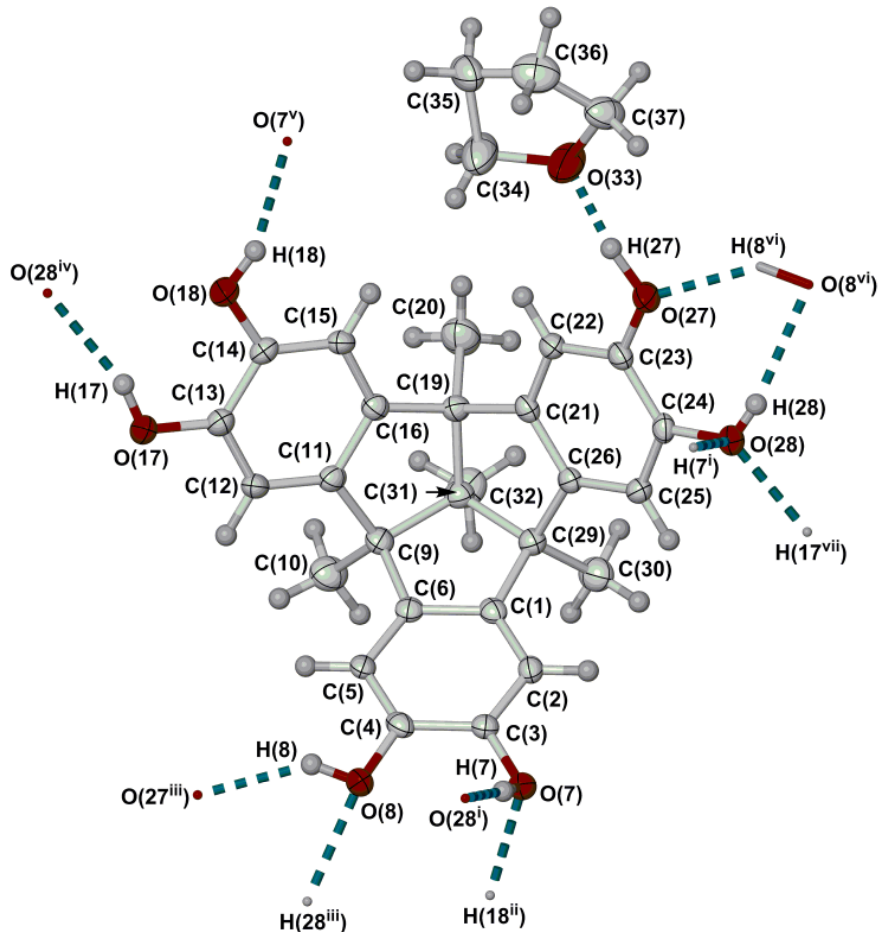


Figure S2. View of the $\text{H}_6\text{tctq}\cdot\text{thf}$ moiety in the structure of $\text{H}_6\text{tctq}\cdot\text{thf}\cdot n\text{MeOH}$. Displacement ellipsoids are at the 50 % probability level, and the partial methanol molecule (which does not form any obvious hydrogen bonds) is not shown. Colour code: C, white; H, pale grey; O, red.

Symmetry codes: (i) $1-x, 2-y, 1-z$; (ii) $x, 1+y, z$; (iii) $1+x, y, z$; (iv) $1+x, -1+y, z$; (v) $x, -1+y, z$; (vi) $-1+x, y, z$; (vii) $-1+x, 1+y, z$.

Table S2 Hydrogen bond parameters in the structure of $\text{H}_6\text{tctq}\cdot\text{thf}\cdot n\text{MeOH}$ (\AA , $^\circ$). See Figure S2 for the atom numbering scheme. Symmetry codes: (i) $1-x, 2-y, 1-z; 1+x, y, z$; (iv) $1+x, -1+y, z$; (v) $x, -1+y, z$; (vi) $-1+x, y, z$.

	O-H	H...O	O...O	O-H...O
O(7)-H(7)...O(28) ⁱ	0.90(5)	1.88(5)	2.776(4)	178(4)
O(8)-H(8)...O(27) ⁱⁱⁱ	0.86(5)	1.95(5)	2.693(3)	144(5)
O(17)-H(17)...O(28) ^{iv}	0.85(6)	2.03(6)	2.859(4)	165(5)
O(18)-H(18)...O(7) ^v	0.85(6)	1.96(6)	2.766(3)	158(5)
O(27)-H(27)...O(33)	1.00(6)	1.60(6)	2.588(4)	172(5)
O(28)-H(28)...O(8) ^{vi}	0.73(5)	2.17(5)	2.882(3)	168(5)

The fractional methanol site C(38)/O(39) does not have an obvious hydrogen-bond acceptor, but is positioned to accept two weak C-H...O interactions from the H_6tctq and thf molecules [$\text{C}(20)\dots\text{O}(39) = 3.34(4)$, $\text{C}(34)\dots\text{O}(39) = 3.26(3)$ \AA].

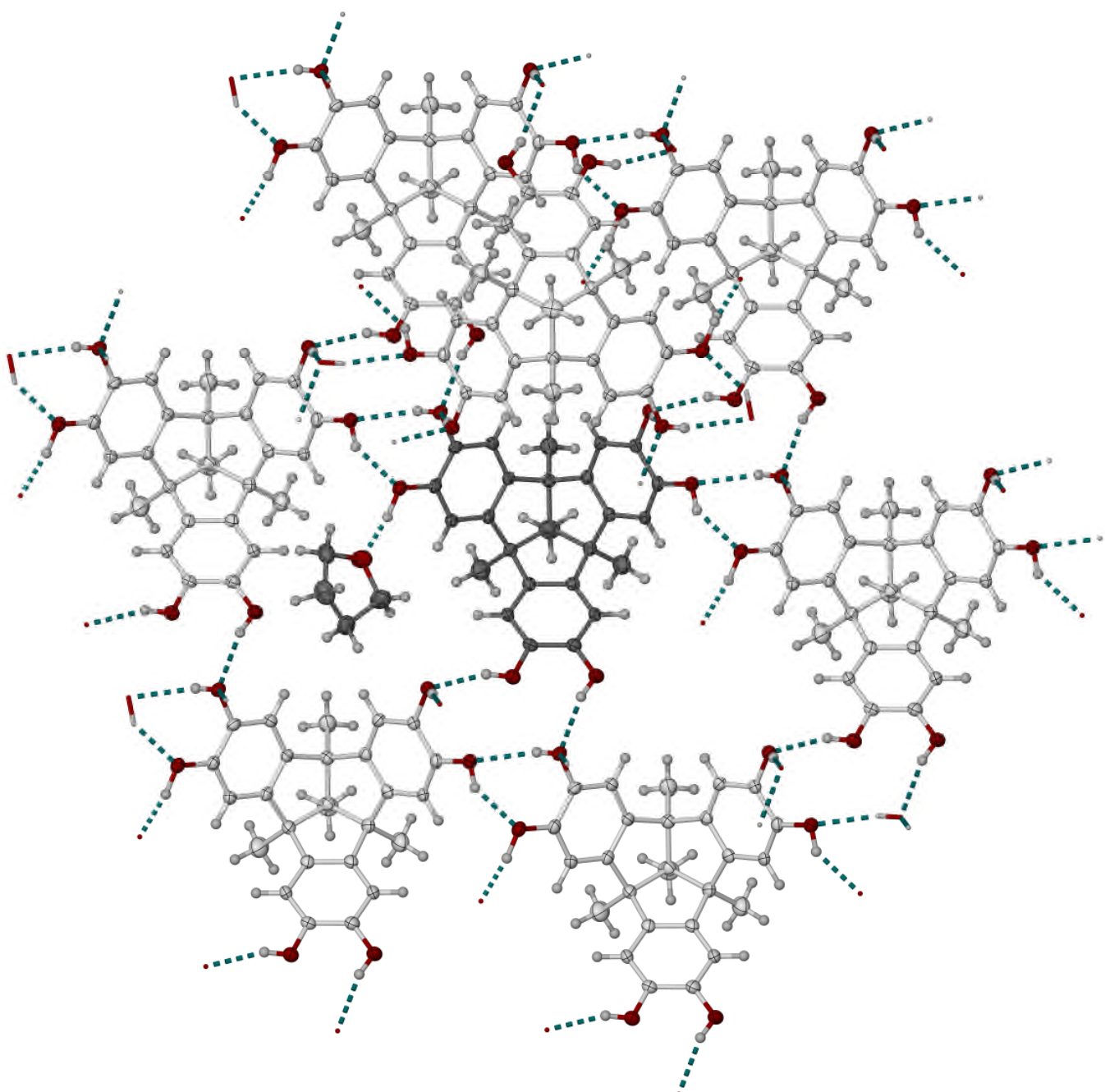


Figure S3. View of the hydrogen bond connectivity in $\text{H}_6\text{tctq}\cdot\text{thf}\cdot n\text{MeOH}$. A central $\text{H}_6\text{tctq}\cdot\text{thf}$ moiety is shown in dark colouration, surrounded by its seven nearest neighbour H_6tctq molecules with paler colouration. Displacement ellipsoids are at the 50 % probability level, and the partial methanol molecule (which does not form any obvious hydrogen bonds) is not shown. Colour code: C, white or dark grey; H, pale grey; O, red.

Six of the seven connected molecules are disposed about the central molecule in an approximately hexagonal arrangement, within the same half of the hydrogen bonded bilayer (Figure S4). An additional connection to a seventh molecule is the link to the other half of the bilayer structure.

The connectivity of the hydrogen bonded bilayers is most simply described as a pair of 2D 6^3 hydrogen bonded sheets, which are linked into bilayers by the seventh connection in the third dimension.

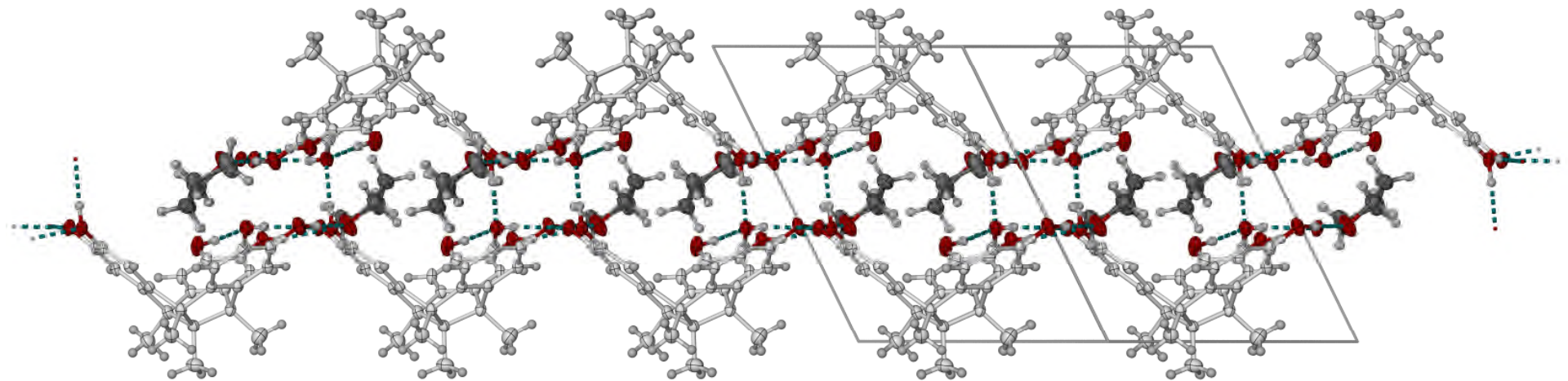


Figure S4. A hydrogen bonded bilayer in the lattice of $\text{H}_6\text{tctq}\cdot\text{thf}\cdot n\text{MeOH}$. The view is parallel to the $(1\bar{1}0)$ crystal vector. Displacement ellipsoids are at the 50 % probability level. The thf molecules are highlighted with dark colouration, and the partial methanol molecule (which does not form any obvious hydrogen bonds) is not shown.

Colour code: C{ H_6tctq }, white; C{solvent}, dark gray; H, pale gray; O, red.

Similar hydrogen bonded bilayer crystal packing is also shown by several solvent clathrates of H_6ctc .^{22,23} The two halves of the bilayer are also linked by inclusion of the thf solvent molecules in the H_6tctq bowl-shaped cavities (Figure S5).

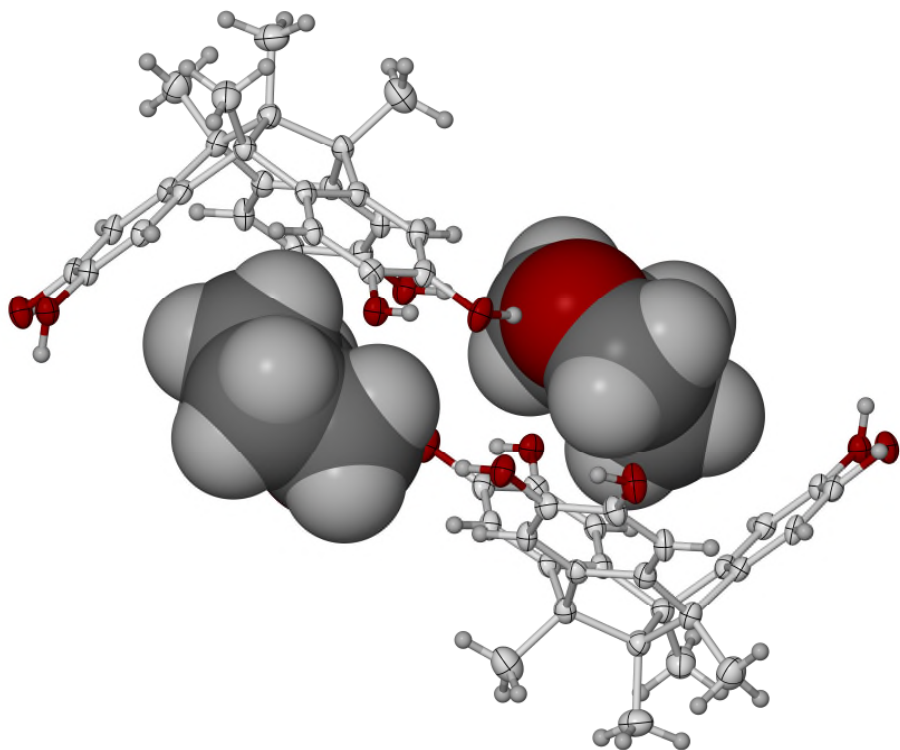


Figure S5. View of the inclusion of thf molecules inside the H_6tctq bowl-shaped cavities in $\text{H}_6\text{tctq}\cdot\text{thf}\cdot n\text{MeOH}$. Each thf molecule is hydrogen bonded to one half of the bilayer structure, and included into the other half. Colour code: C{ H_6tctq }, white; C{solvent}, dark gray; H, pale gray; O, red.

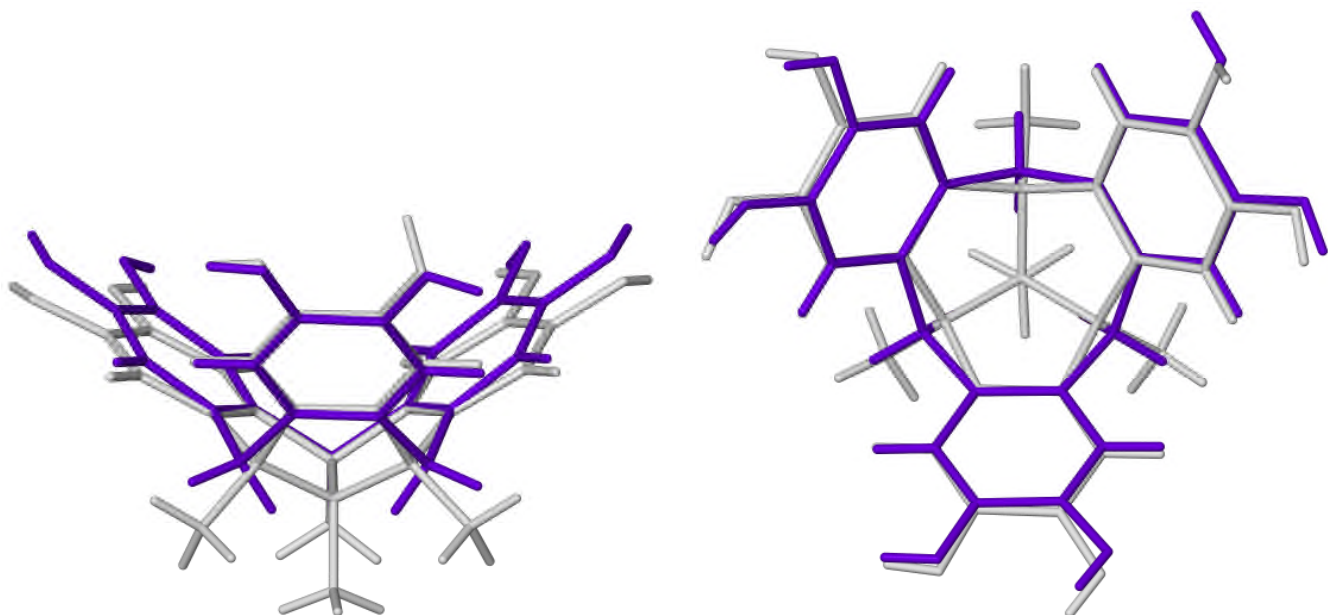


Figure S6. Overlays of the crystallographic molecular structures of H_6tctq (white) and H_6ctc (purple), showing the shallower bowl-shaped conformation of the H_6tctq macrocycle. The left view is the same as Figure 3 of the main article.

The H_6ctc molecule in the Figure is from $\text{H}_6\text{ctc}\cdot 5\text{dmso}$.²³

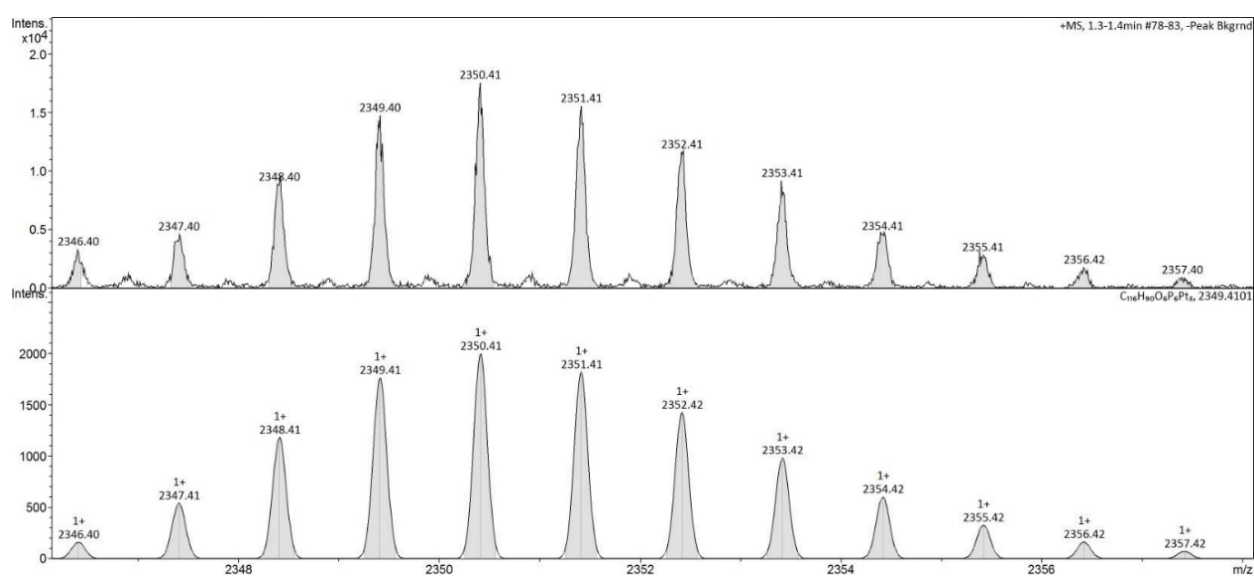
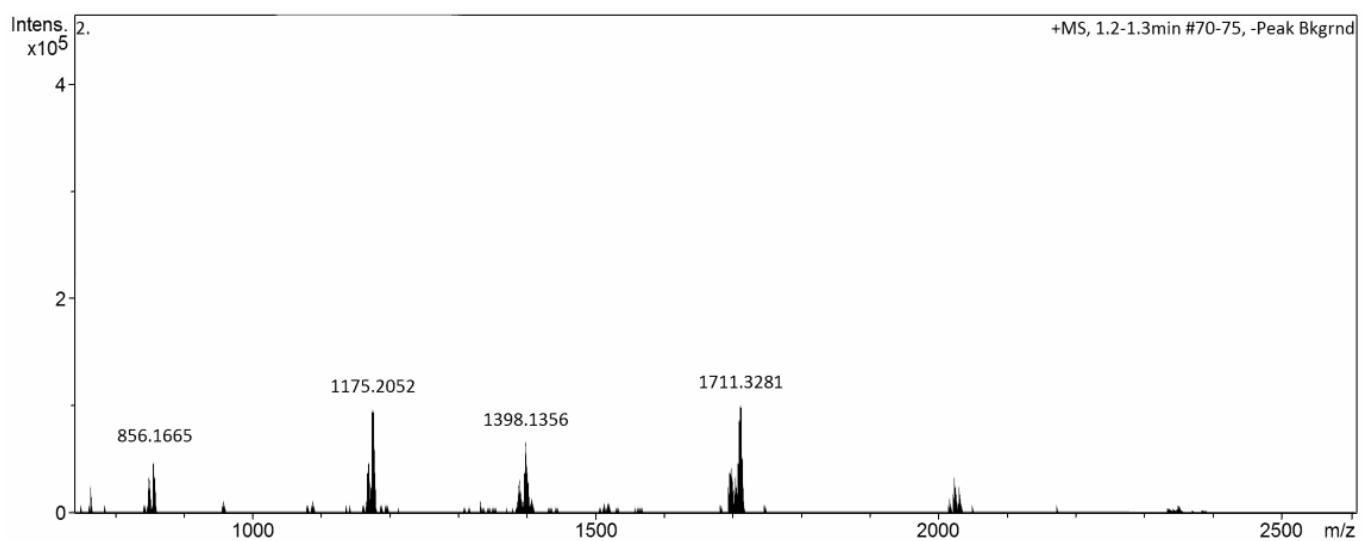


Figure S7. Top: the high-nuclearity species in the high-resolution electrospray mass spectrum of **2a** (more intense mononuclear fragments at lower mass are not shown). Bottom: the observed and simulated molecular ion for the intact $\{[\text{Pt}(\text{dppb})]_3(\text{tctq})+\text{H}\}^+$ molecular ion. Other peak assignments are listed in the Experimental Section.

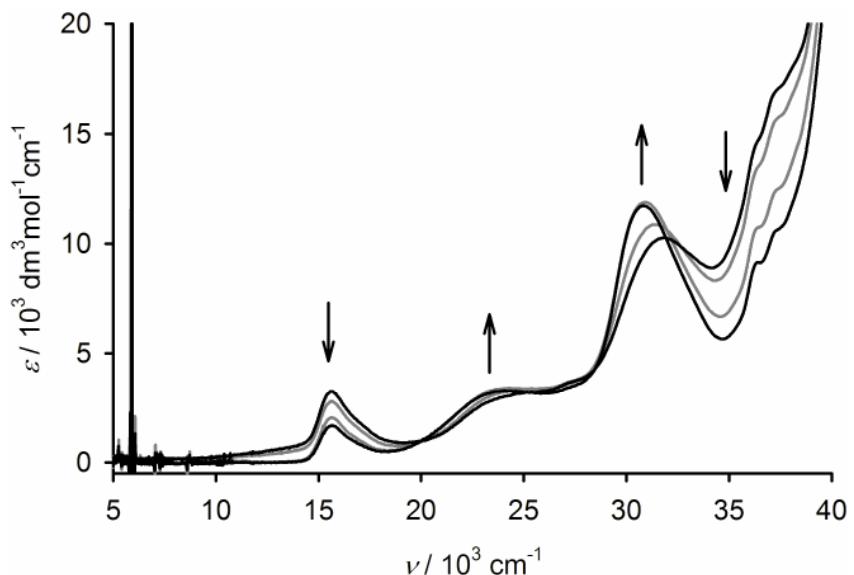


Figure S8. The $\mathbf{2a} \rightarrow [\mathbf{2a}\cdot]^+$ oxidation in CH_2Cl_2 , monitored by titration with $[\text{FeCp}_2]\text{PF}_6$ at 298 K with UV/vis/NIR spectroscopy. The starting and final spectra are highlighted in black while the intermediate spectra are paler.

Although the reaction is not isosbestic under these conditions, the spectral changes during the reaction broadly resemble those in the spectroelectrochemical oxidation (Figure 2, main article). This includes the absence of the IVCT absorption below $10 \times 10^3 \text{ cm}^{-1}$ which is shown by $[\mathbf{1a}\cdot]^+$.²⁴

The exception to the above statement is the feature near $16 \times 10^3 \text{ cm}^{-1}$, which is not present in the spectroelectrochemical data and is of uncertain origin. While $[\text{FeCp}_2]\text{PF}_6$ exhibits an absorption near that energy,²⁵ that assignment is unlikely since the peak is also observed in the starting **2a** spectrum.

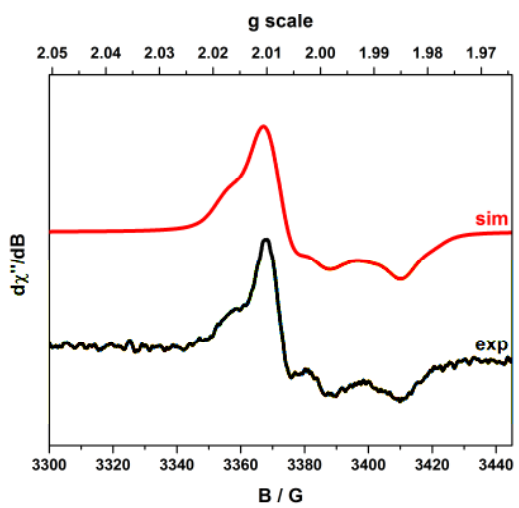


Figure S9. Measured (black) and simulated (red) X-band EPR spectrum of $[2\mathbf{a}^\bullet]^+$ in CH_2Cl_2 solution at 150 K.

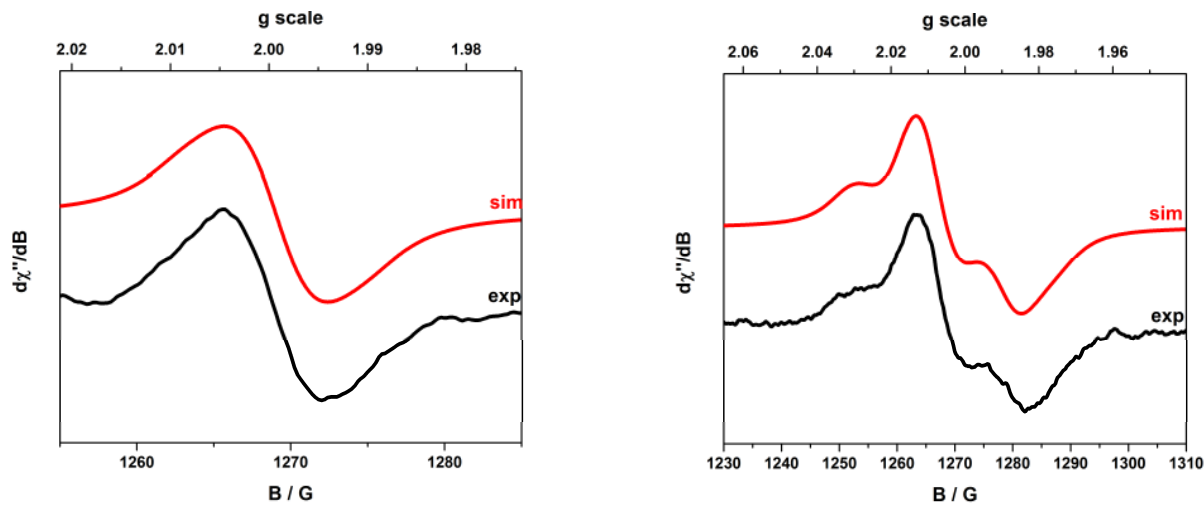


Figure S10. Measured (black) and simulated (red) S-band EPR spectra of $[2\mathbf{a}^\bullet]^+$ in CH_2Cl_2 solution at 300 K (left) and 45 K (right).

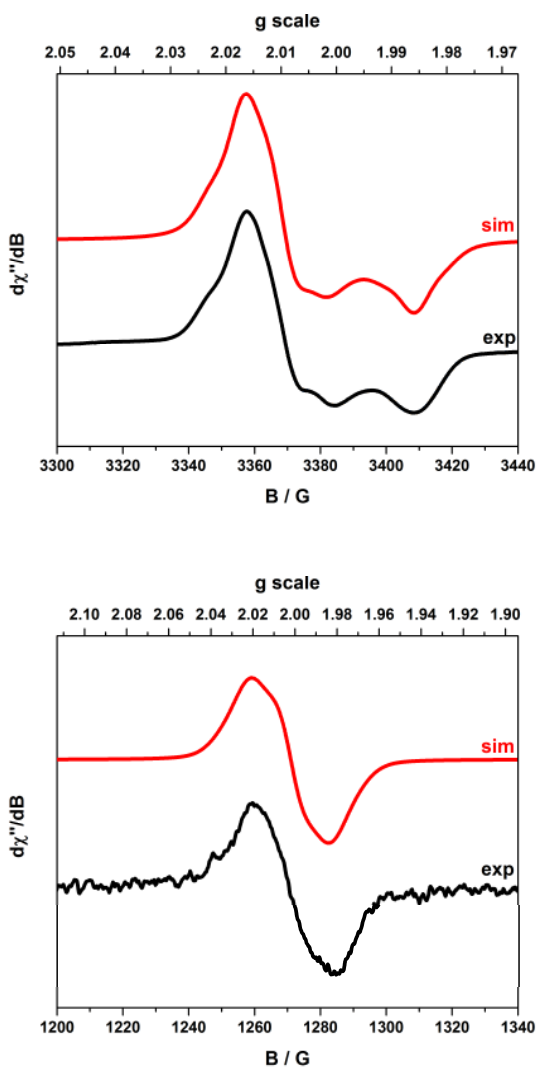


Figure S11. Measured (black) and simulated (red) EPR spectra of $[2\mathbf{b}^\bullet]^+$ in CH_2Cl_2 solution. Top, X-band spectrum at 150 K; bottom, S-band spectrum at 45 K (frozen solution).

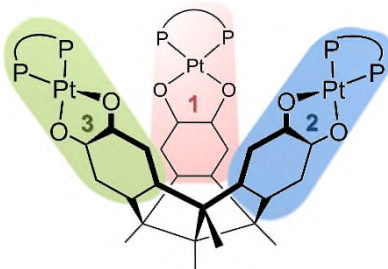
A spectrum of this radical in fluid solution was not achieved, because of its instability towards decomposition at elevated temperatures.

Table S3 Simulated EPR parameters for $[2\mathbf{a}^\bullet]^+$ and $[2\mathbf{b}^\bullet]^+$ in CH_2Cl_2 solution (Figures S9-S11).

	T / K	g_1	g_2	g_3	$A_1\{\text{Pt}\} / 10^{-4} \text{ cm}^{-1}$	$A\{\text{P}\} / 10^{-4} \text{ cm}^{-1}$
$[2\mathbf{a}^\bullet]^+$	300	2.006	—	—	20	5
	45	2.010	2.006	1.984	60	8
$[2\mathbf{b}^\bullet]^+$	150	2.016	2.009	1.985	60	7

These parameters resemble those of $[1\mathbf{a}^\bullet]^+$ ²⁴ and other platinum(II)/semiquinonate radical species.²⁶

Table S4 Calculated mean bond distances (\AA) and angles ($^\circ$) in the different oxidation states of **2a**. Data in square brackets are from the corresponding calculation of **1a** $^{z+}$ in ref. 24. Relevant experimental data from **1a/1b** are also listed in ref. 24.



	$\{ \text{Pt}(\text{dppb}) \}_3(\mu_3\text{-tctq})]^{z+}$	$z = 0$ $M_S = 1$	$z = 1$ $M_S = 2$	$z = 2$ BS(1,1) $M_S = 3$	$z = 3$ BS(2,1) $M_S = 2$
1	Pt–P	2.242 [2.221]	2.244 [2.232]	2.247 [2.228]	2.251 [2.234]
	Pt–O	2.018 [2.015]	2.035 [2.054]	2.054 [2.055]	2.081 [2.081]
	C–O	1.361 [1.363]	1.342 [1.337]	1.327 [1.327]	1.308 [1.308]
	C–C _{arom}	1.409 [1.405]	1.413 [1.412]	1.416 [1.413]	1.421 [1.418]
	τ^a	1.1 [0.4]	1.7 [1.3]	1.7 [2.2]	1.5 [0.4]
	α^b	54.1 [56.5]	45.1 [55.9]	47.8 [58.9]	49.7 [60.8]
	θ^c	0.8 [0.4]	3.4 [2.8]	4.3 [4.9]	5.1 [4.9]
2	Pt–P	2.242 [2.221]	2.244 [2.232]	2.247 [2.228]	2.251 [2.234]
	Pt–O	2.019 [2.017]	2.033 [2.047]	2.056 [2.056]	2.082 [2.080]
	C–O	1.361 [1.364]	1.346 [1.347]	1.326 [1.326]	1.308 [1.308]
	C–C _{arom}	1.409 [1.405]	1.412 [1.410]	1.417 [1.413]	1.421 [1.418]
	τ^a	0.9 [0.5]	0.9 [0.4]	1.2 [2.5]	1.6 [0.3]
	α^b	53.4 [56.5]	55.6 [55.9]	54.6 [58.9]	56.0 [60.8]
	θ^c	0.5 [0.7]	1.4 [1.4]	4.1 [4.3]	5.5 [1.8]
3	Pt–P	2.242 [2.221]	2.244 [2.232]	2.247 [2.229]	2.251 [2.234]
	Pt–O	2.017 [2.017]	2.033 [2.047]	2.056 [2.056]	2.082 [2.081]
	C–O	1.360 [1.364]	1.346 [1.346]	1.326 [1.326]	1.308 [1.308]
	C–C _{arom}	1.409 [1.405]	1.412 [1.410]	1.417 [1.413]	1.421 [1.418]
	τ^a	0.8 [0.5]	0.8 [0.4]	1.3 [2.2]	1.5 [0.3]
	α^b	49.1 [56.5]	55.0 [55.9]	53.9 [58.9]	54.8 [60.8]
	θ^c	1.4 [0.7]	1.4 [1.4]	4.2 [5.5]	5.3 [2.2]
	Pt…Pt	10.57 [10.37]	10.16 [10.33]	10.43 [10.62]	10.80 [10.62]
		10.14 [10.37]	10.84 [10.33]	10.84 [10.69]	11.11 [10.83]
		10.20 [10.52]	10.11 [10.58]	10.38 [10.69]	10.72 [10.88]
	Average	10.30 [10.42]	10.37 [10.41]	10.55 [10.67]	10.88 [10.78]

^aDihedral angle between $\{ \text{PtO}_2 \}$ and $\{ \text{PtP}_2 \}$ mean planes. ^bAngle between $\{ \text{PtO}_2 \text{C}_6 \}$ plane and molecular C_3 axis. ^cDihedral angle between $\{ \text{PtO}_2 \}$ and $\{ \text{O}_2 \text{C}_6 \}$ mean planes.

Table S5 Geometry optimized coordinates for **2a**.

Pt	5.24599651944574	-2.82177386034587	-0.41889214504644
Pt	0.06201213565145	5.88762465510134	-0.39373685626443
Pt	-5.32604056080638	-2.76784024015213	-0.40959795736022
P	7.23282918755966	-2.14839425926704	-1.20765986253635
P	5.60830463272476	-4.72341057948104	-1.54915019635748
P	-1.45041234302043	7.14789163285633	-1.46545166635659
P	1.61329655939562	7.15123458806947	-1.40438633766257
P	-5.72369839978210	-4.67560603371592	-1.51751562032226
P	-7.30659269342503	-2.07256356356474	-1.19490555934082
O	4.88421206909552	-1.12541852859956	0.61174843560563
O	3.46648511092363	-3.39667533526150	0.34128641533946
O	-1.30053680594094	4.72004827649853	0.52649534616711
O	1.38964624501313	4.71405319811726	0.56882305411961
O	-3.55426293608222	-3.36347895742401	0.35120931346178
O	-4.93421020634811	-1.06693784374143	0.60135151329998
C	1.24259933101437	-1.51496143356515	2.59211624050080
C	1.97932314891001	-0.32508652448230	2.72477006431035
C	3.21233936741285	-0.16378159041510	2.07040903200077
C	3.69504891148397	-1.21156359920998	1.26674450766992
C	2.94448794058455	-2.41299687217337	1.12352087468409
C	1.71628960707435	-2.56780247519595	1.79058883179084
C	-0.03053107237560	-1.50466721078106	3.42849920736962
C	-1.29744558511201	0.72083061025956	3.58311244207936
C	1.27285084206667	0.69917927993834	3.60239799013421
C	0.70591665186236	1.83625110127308	2.75983215123942
C	-0.69872512581698	1.84262533854784	2.74198900814242
C	-1.40459662503568	2.80562506176839	2.00057491022214
C	-0.68105756210719	3.76432428756111	1.27053680635594
C	0.74278370938125	3.76051758039889	1.29211418150746
C	1.43896503350166	2.79521895442630	2.03986053460073
C	-2.01753279079755	-0.29644945807164	2.70907104031691
C	-1.30178270921566	-1.50048480551764	2.58926496886365
C	-1.79220035822139	-2.55195494811404	1.7960506329882
C	-3.01623222883612	-2.38174880579993	1.12498075325567
C	-3.74623492995963	-1.16652624563788	1.25653058512641
C	-3.24630234256113	-0.11963474466556	2.05079190730067
C	7.99886808643976	-3.47746144567494	-2.22737894114046
C	7.24886848860444	-4.66612637530471	-2.38538749945823
C	7.76889837354339	-5.72958061095402	-3.14769768912409
C	9.03475005472093	-5.60587871023063	-3.74663298475410
C	9.78029638068891	-4.42549069435378	-3.58895585951734
C	9.26512482706351	-3.35875112349055	-2.83154734639783
C	-0.60571184600960	8.40916276196560	-2.50950673227454
C	0.80840215850383	8.41100600702654	-2.48092456243499
C	1.52615771334328	9.34740517623379	-3.24962146584842
C	0.83289965269830	10.27776490455761	-4.04383421686330
C	-0.57178477512504	10.27540843423777	-4.07278111083412
C	-1.29416545035673	9.34297051021830	-3.30756383770985
C	-7.37305912014432	-4.60640469570337	-2.33536305575101
C	-8.10431658228646	-3.40515575040346	-2.18522531909368
C	-9.37635833546561	-3.27726739617903	-2.77511072077121
C	-9.91604241317296	-4.34743804525398	-3.51021411520439
C	-9.18900779618720	-5.54023609758904	-3.66035845406858
C	-7.91739184944702	-5.67307751439054	-3.07584065810099
C	-0.03706065426931	-2.72075991141926	4.37974313421629
C	2.22292552970509	1.25459283231615	4.68108217756119
C	-2.24574583997833	1.30517655087375	4.64817435993735
H	7.31982577480181	-0.99625167628883	-2.05741699887057
H	4.72222476432564	-5.11397983512613	-2.60729206548768
H	-2.39804300189164	7.92897274721516	-0.72418941056967
H	2.56775211517151	6.53624249392106	-2.28051405423642
H	-4.85469874399604	-5.08787370651935	-2.58160863217753
H	-7.38185302407129	-0.93375061215390	-2.06384360585364
H	3.81209842834241	0.75301914094252	2.16605652326956
H	1.16377773871478	-3.51136527096036	1.67369868311094
H	-2.50414496311906	2.82792384096792	1.96154469689442
H	2.53930752959441	2.81017612176780	2.03082582225156

H	-1.25663917201981	-3.50642696897758	1.68938655542717
H	-3.83139939186586	0.80737839428755	2.13870587596433
H	7.18795715284579	-6.65660115351044	-3.27302089615510
H	9.44159471048416	-6.43950278393151	-4.33878247978319
H	10.77160037114235	-4.33461734544459	-4.05719306544790
H	9.85241897941875	-2.43517945181466	-2.70962255876846
H	2.62776149212418	9.35281618102982	-3.22904162940044
H	1.39491935390726	11.01005859184384	-4.64321252447247
H	-1.11120517749142	11.00578314354392	-4.69487567651913
H	-2.39566184591288	9.34450747979167	-3.33284639465212
H	-9.94930327673686	-2.34394018037660	-2.65914526497148
H	-10.91203044455453	-4.24939640034796	-3.96687702712641
H	-9.61498555052373	-6.37645889045624	-4.23509633890257
H	-7.35096778048741	-6.60983208308981	-3.19517436024237
H	-0.93954710473574	-2.73560919323297	5.02309696096555
H	0.86519380338461	-2.74399430668349	5.02321206505179
H	-0.04103489627408	-3.65808944306343	3.78735321376806
H	-1.72476332394750	2.03554360588969	5.29866506404304
H	-2.69506442292126	0.51294560448851	5.27984279199579
H	-3.07979472591929	1.84550287120236	4.15581094864016
H	1.71108748307111	1.99039845990301	5.33257995611464
H	3.07335119115857	1.78084573197247	4.20163265716550
H	2.64843565616853	0.44736715238972	5.30990435647890
C	-0.02295849475037	-0.07041883299874	4.14475433223417
C	-0.03596715686693	-0.18765248992243	5.66958628033154
H	-0.02991715943626	0.80444979449085	6.15930763752350
H	0.84742741632006	-0.74160586288496	6.04073974363138
H	-0.93608298735865	-0.72405944904081	6.02625412133965
H	-2.36809317706747	6.53121285796942	-2.37882364321572
H	2.52932520110321	7.93359349077095	-0.62576595854193
H	5.64508299494609	-5.97332679543556	-0.84836100011723
H	8.27892618387880	-1.80160189011344	-0.29077362562948
H	-5.76786650913263	-5.91772018099791	-0.80342441113883
H	-8.33724478134954	-1.69140240713228	-0.27421637780562

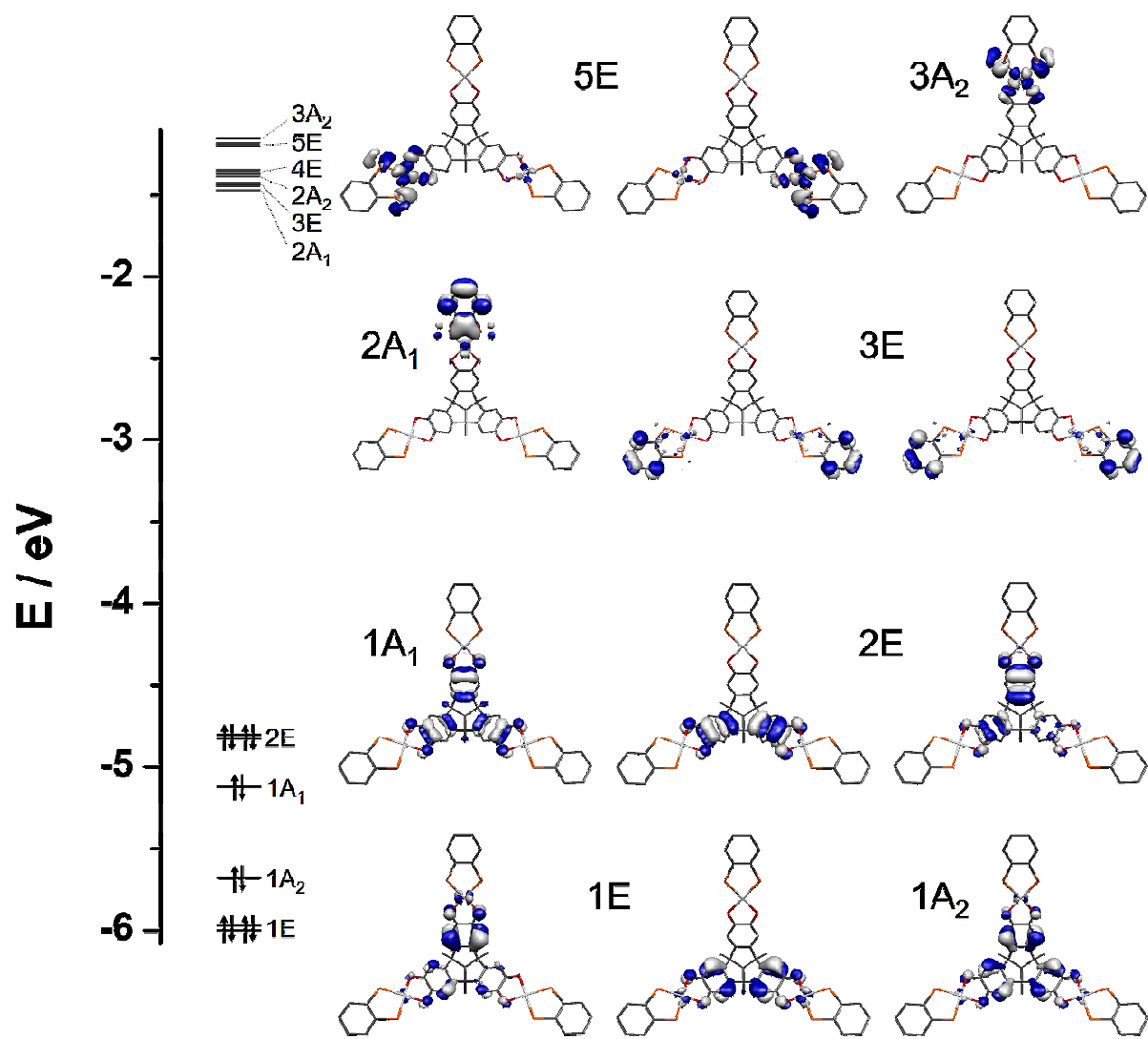


Figure S12. MO energy level scheme of frontier Kohn-Sham orbitals for **2a** with C_{3v} symmetry labels.

Table S6 Geometry Optimized Coordinates for [2a[•]]⁺

Pt	5.37997534203993	-2.84554034086670	-0.38248926581373
Pt	0.05271272730177	5.74572539411352	-0.68352881327806
Pt	-5.45849987323997	-2.77879153758979	-0.36646019458886
P	7.42423787985497	-2.2116855940339	-1.05292979897718
P	5.76631604513920	-4.74855938713029	-1.50792465712083
P	-1.46480898910844	7.09539170353490	-1.63873898787136
P	1.59912018215504	7.08783291389820	-1.60238582798799
P	-5.87981144984886	-4.68197314755156	-1.47916948251561
P	-7.49282865752913	-2.11350145173619	-1.03710913549258
O	4.99088915622314	-1.14517721295867	0.65780814051370
O	3.53074048416026	-3.37767530529859	0.27710162530957
O	-1.30743076128404	4.52451828185117	0.21052600259334
O	1.38567479842797	4.51701926469779	0.24034866713728
O	-3.61844470436527	-3.33916161776508	0.29566988311572
O	-5.03841333262604	-1.07819883044803	0.66087984196509
C	1.25856752412775	-1.50092224579292	2.45172844569804
C	2.02231462327904	-0.32823156133008	2.64807481263785
C	3.28358978777333	-0.17520805908331	2.05344713081275
C	3.78268224979895	-1.21583114260535	1.24875841390520
C	3.00541042731048	-2.40741107711089	1.04563014584468
C	1.74180098091328	-2.54732855483147	1.65730520950577
C	-0.02543107067603	-1.49034610798490	3.26844090512153
C	-1.29251931751433	0.72027726008937	3.47607539140155
C	1.27829616745166	0.69909428476835	3.48851549080548
C	0.71515578847471	1.75432263249700	2.54651793623154
C	-0.70319203172429	1.76052696118858	2.53346518601375
C	-1.41275806984621	2.67465601750807	1.74375208205530
C	-0.69288960260527	3.60159424020636	0.96721310144788
C	0.74930686461268	3.59729799543839	0.98282396573793
C	1.44681915756556	2.66467243659496	1.77267870350034
C	-2.05416727459607	-0.29893363481370	2.64244626202007
C	-1.31156511649777	-1.48646669729872	2.45499624138240
C	-1.81414914949861	-2.53037423601273	1.66916185270795
C	-3.07539502296040	-2.37263678867213	1.05683956009036
C	-3.83105002662223	-1.16602279950350	1.25130360862591
C	-3.31292557592280	-0.12821576859515	2.04759471472851
C	8.20946097735750	-3.54120711277063	-2.05187449482764
C	7.44391080989138	-4.71228672683283	-2.26271677891745
C	7.97760174475637	-5.77544549819606	-3.01520889597251
C	9.27016916421940	-5.66811786012902	-3.55262702665137
C	10.03134704470479	-4.50453107067251	-3.34260180169798
C	9.50451703935728	-3.43971838498989	-2.59394232600708
C	-0.62693990131031	8.51312162780325	-2.45848570545056
C	0.78796577119315	8.51013165211250	-2.44084578587613
C	1.50158823771636	9.56330461357691	-3.04292447762549
C	0.80333551233329	10.61560892649166	-3.65626465650043
C	-0.60283466521952	10.61845800731349	-3.67405083296778
C	-1.32072385876235	9.56917675606067	-3.07849637430118
C	-7.55968661115113	-4.62304961340396	-2.22747874977819
C	-8.30451728653948	-3.43768499588939	-2.02251142351552
C	-9.59997236017454	-3.31858683590050	-2.55993547162246
C	-10.14791207897365	-4.38012083100914	-3.29795937154526
C	-9.40736101695960	-5.55790329629111	-3.50218353146129
C	-8.11444658122356	-5.68277363818884	-2.96948513609163
C	-0.02934110787966	-2.72723112211193	4.20182272508665
C	2.17440894610317	1.34140236878593	4.55928504904669
C	-2.18025338503950	1.38886656584653	4.53799655695144
H	7.54949677128460	-1.04262843560946	-1.86893848823108
H	4.90592524341583	-5.09934708526694	-2.59647100682306
H	-2.44517457214957	7.70367556801671	-0.79372392999854
H	2.48129243527919	6.55362285105280	-2.59545263390852
H	-5.02941504450311	-5.05215750941364	-2.56911258900806
H	-7.59985124271371	-0.94972131318661	-1.86255638726169
H	3.90136093759355	0.72137851711929	2.20436125252793
H	1.17995201921558	-3.47905223501350	1.50074779637804
H	-2.51174676203894	2.70316327000791	1.71859013165437

H	2.54623224806602	2.68545533767519	1.76879743523842
H	-1.26930291530377	-3.47323228549685	1.51937681643905
H	-3.91499871748902	0.77997449675869	2.19256624829309
H	7.38698001450147	-6.68960610484518	-3.18203053551237
H	9.68747559620727	-6.50058031582108	-4.13861452694864
H	11.04411588680782	-4.42687256758341	-3.76432803711287
H	10.10580033823802	-2.53148638781666	-2.43197648047127
H	2.60298925649336	9.56736221610056	-3.03153286343049
H	1.36047812775571	11.44189752037190	-4.12263380883286
H	-1.14471090571862	11.44696952621876	-4.15431378537058
H	-2.42202526809233	9.57775307925394	-3.09526570675491
H	-10.18528360969204	-2.39916770811548	-2.40250584392488
H	-11.16114195484962	-4.28867209360688	-3.71576756779223
H	-9.84118775883120	-6.38776008527758	-4.07978556172679
H	-7.53999478666129	-6.60799797892142	-3.13173702015156
H	-0.93014034668273	-2.75029641089626	4.84549542680246
H	0.87377471788366	-2.75786826800448	4.84196389872791
H	-0.03410284254169	-3.65341046562523	3.59364466859282
H	-1.61346352164181	2.13280255598513	5.13201566148238
H	-2.62805682088589	0.64523077738690	5.22638973894956
H	-3.01517715446264	1.93067649476148	4.05001767984788
H	1.61925639206596	2.09167965678160	5.15612291357777
H	3.02274436750807	1.87024886555569	4.08014538568998
H	2.60344228453843	0.58324680986830	5.24361527198264
C	-0.01623548733988	-0.07444022205865	4.02008527212490
C	-0.02567922658851	-0.22104359511469	5.54186876040618
H	-0.02055828920699	0.76227664278371	6.04731465631175
H	0.85962265512728	-0.77893711317768	5.90131101040014
H	-0.92413814533324	-0.76453327002209	5.89074548349030
H	-2.32553708477881	6.56437237554466	-2.65212059381644
H	2.56184003984675	7.69019423536333	-0.73312757226443
H	5.73668069170468	-5.98347254553139	-0.78682489208182
H	8.40025333657773	-1.90145199936931	-0.05418688606106
H	-5.86703565074201	-5.91340250854729	-0.75163016331677
H	-8.46006224740691	-1.77790319589339	-0.03814736965469

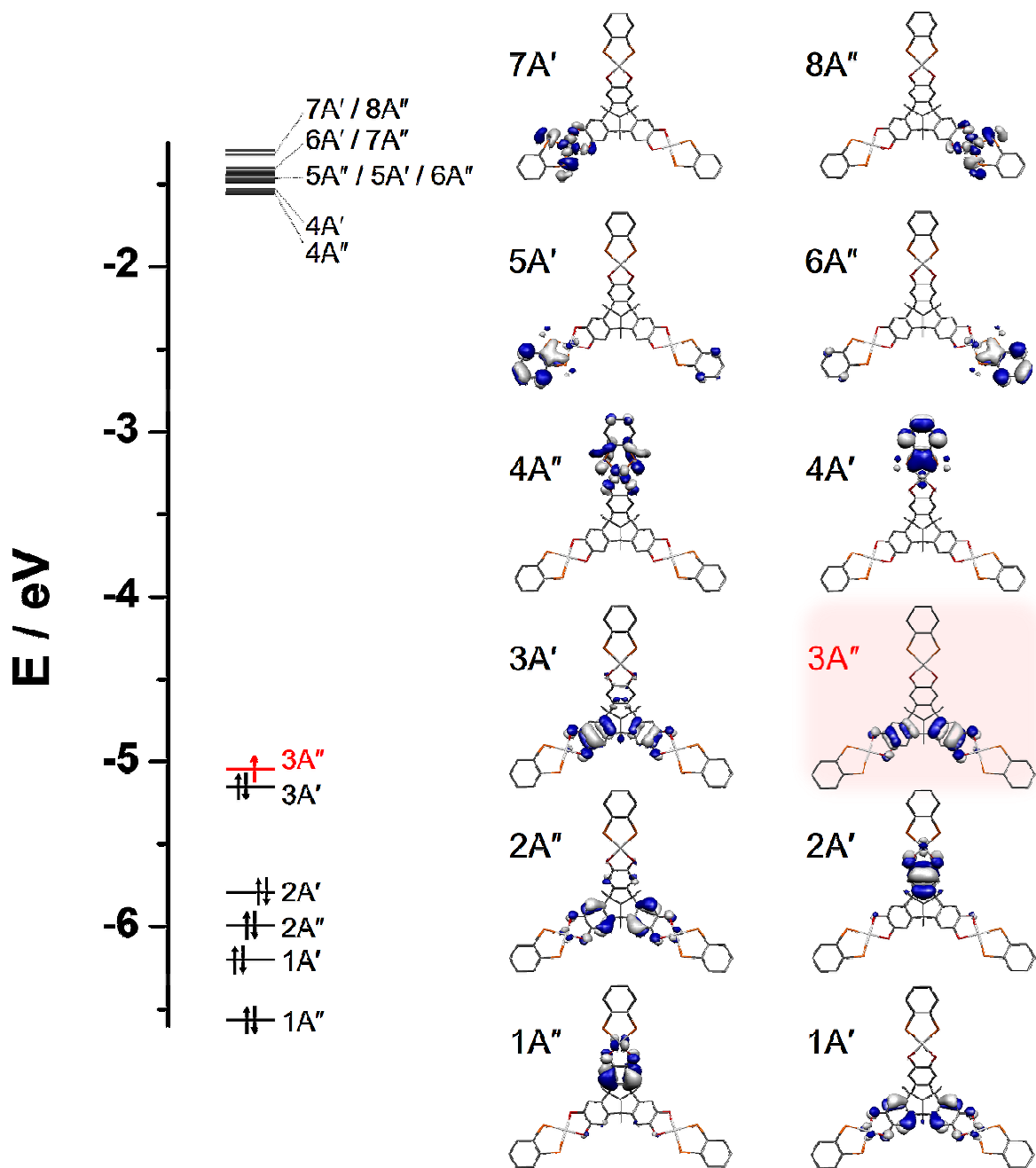


Figure S13. MO energy level scheme of frontier Kohn-Sham orbitals for $[2a\cdot]^+$ with C_s symmetry labels.

Table S7 Geometry Optimized Coordinates for [2a[•]]²⁺

Pt	5.37881192726361	-2.93161915560328	-0.48148668126795
Pt	0.05491346040035	5.97829545486790	-0.63739277879165
Pt	-5.46295135619219	-2.86769094674581	-0.45323216225532
P	7.45771172647013	-2.35089808368056	-1.10539272814045
P	5.80412845370965	-4.90108108477036	-1.47692547557739
P	-1.46285260989665	7.38664089318741	-1.51071701130788
P	1.59803085287425	7.38173613728719	-1.47346454577548
P	-5.92546156517615	-4.83615717963647	-1.43422496463502
P	-7.53066351807131	-2.25241098727607	-1.08128212038402
O	4.93657674522701	-1.16408511657774	0.46858788573120
O	3.48287342748572	-3.40814742649530	0.15611430578663
O	-1.30441736115251	4.68038010124024	0.19127672879872
O	1.38785982955498	4.67486123338300	0.22522924345550
O	-3.57493986662749	-3.37386533330786	0.18613746665193
O	-4.98584071047271	-1.09998556476813	0.47962172816737
C	1.23370626303014	-1.49001340030424	2.28749913392223
C	1.99298405137134	-0.29179659911929	2.43164656903640
C	3.24313395660740	-0.14835665313608	1.82765941087933
C	3.74554584693394	-1.21445234424276	1.04815912028246
C	2.96045531096891	-2.42903834163471	0.88125615387469
C	1.70201458933345	-2.55251552140716	1.51323718668489
C	-0.02378611653310	-1.47052504281962	3.14312915681172
C	-1.28928647789472	0.75286650900244	3.28605590017266
C	1.27918566614847	0.73154224072385	3.29894366084786
C	0.72015401957082	1.81867610430356	2.39042831412302
C	-0.70331413993116	1.82427769939113	2.37580785598095
C	-1.41519277856540	2.76687456512719	1.63125512064147
C	-0.69643541196781	3.73415768067653	0.89460544652406
C	0.75844855444976	3.73082958961201	0.91246006776583
C	1.45442702718909	2.75842560570059	1.66417634702411
C	-2.02200080954320	-0.26358414711356	2.42729870533666
C	-1.28525687924539	-1.47702840904104	2.29336711523819
C	-1.77527191330668	-2.53831319415294	1.53097702664890
C	-3.03267107010280	-2.39755016466250	0.90032303867297
C	-3.79454466278567	-1.16686734411304	1.05675498368793
C	-3.27055182899790	-0.10272660599901	1.82467313251076
C	8.27877816653796	-3.74626807768994	-1.96729117249247
C	7.51406447185165	-4.92484085524358	-2.13994561776454
C	8.07515042822265	-6.04064903441580	-2.78875476101734
C	9.39550945406323	-5.97550252841693	-3.26103044370569
C	10.15563064515694	-4.80447761635782	-3.08932509823872
C	9.60181588166115	-3.68744742319548	-2.44372607477941
C	-0.62870500851069	8.83681193167389	-2.26283537789678
C	0.78669275566887	8.83483027521801	-2.24507729394160
C	1.50050350887008	9.91319713343198	-2.80021987378605
C	0.79927533254036	10.98862139186975	-3.36820398233835
C	-0.60719818191123	10.99047604751692	-3.38602278476852
C	-1.32541861969811	9.91699860029743	-2.83591779990182
C	-7.63348591152604	-4.83028886235266	-2.10251573464320
C	-8.37556400647726	-3.63609318266438	-1.93894711936199
C	-9.69577323419399	-3.55429944184804	-2.41974992149923
C	-10.26936385648436	-4.66403359722707	-3.06057351781108
C	-9.53177744117055	-5.85061302487903	-3.22320214837670
C	-8.21435808435532	-5.93870450515011	-2.74654913814972
C	-0.02595592031317	-2.68292237574850	4.09857001087588
C	2.21384984048616	1.33619469363227	4.36144943321085
C	-2.21531524013387	1.38650352100692	4.33950570423099
H	7.59152696313611	-1.23113389673020	-1.98283860863648
H	4.96754530081347	-5.27528639663938	-2.57316002196015
H	-2.42569231700966	7.92774631869388	-0.60474162132109
H	2.48393320248471	6.87049334137824	-2.47238831620389
H	-5.09321985745550	-5.23460278141838	-2.52510382052101
H	-7.64391988493892	-1.13328797624219	-1.96241839046113
H	3.86488169507061	0.74799693271014	1.95767112106707
H	1.15406145688682	-3.49886125546482	1.40852151700538
H	-2.51377412812185	2.80653806032244	1.61656676000099

H	2.55328451240897	2.79146024043889	1.67398722735074
H	-1.24554536843557	-3.49583696304699	1.43448231687341
H	-3.87556339957283	0.80590835583114	1.94833452045006
H	7.48796212806683	-6.96176401487520	-2.92648459938610
H	9.83595882848054	-6.84768574992101	-3.76634971519115
H	11.18979584475514	-4.76176524792052	-3.46082416452198
H	10.20407921420136	-2.77522991127321	-2.31145581975764
H	2.60172621880307	9.92040597396925	-2.78908882868647
H	1.35480494983816	11.83465466382617	-3.79944128146803
H	-1.14943567353964	11.83795975760607	-3.83115831576873
H	-2.42653856878390	9.92703192986266	-2.85291899854572
H	-10.28060287000623	-2.62979769514656	-2.29455829705109
H	-11.30145521557005	-4.60333563573364	-3.43526935004046
H	-9.98768619740717	-6.71701709183475	-3.72471402434496
H	-7.64484324008527	-6.87188768136247	-2.87710122304930
H	-0.92405171063047	-2.68918365026485	4.74600974623930
H	0.87651181176178	-2.69636891482811	4.73983937318945
H	-0.03126038437533	-3.62616034515502	3.51737851585468
H	-1.67299260636477	2.12875389693274	4.95614813588326
H	-2.65959521531049	0.62225149980067	5.00615835845921
H	-3.05121517630255	1.92129351850388	3.84647923651106
H	1.68401387139301	2.08369509533799	4.98242012764593
H	3.06310916970586	1.85806254224719	3.87734291563052
H	2.63871892416310	0.55641433336309	5.02245054438357
C	-0.01435303619044	-0.03271599097675	3.85189960631751
C	-0.02359842716641	-0.14005811141362	5.37695438857218
H	-0.01739420236454	0.85353538575917	5.86116606577047
H	0.86027729719014	-0.69024849919423	5.74970261693125
H	-0.92144923543320	-0.67438092440396	5.73944406690272
H	-2.32634906811752	6.87739451999450	-2.53002905186507
H	2.54088790287959	7.92002760496220	-0.54504333614441
H	5.69714889088270	-6.06882594367992	-0.66145449227866
H	8.35301076345009	-1.96915653539997	-0.06019775597978
H	-5.84424516183581	-5.99994045551888	-0.61006443337988
H	-8.41999605476459	-1.85183459044906	-0.03808241344341

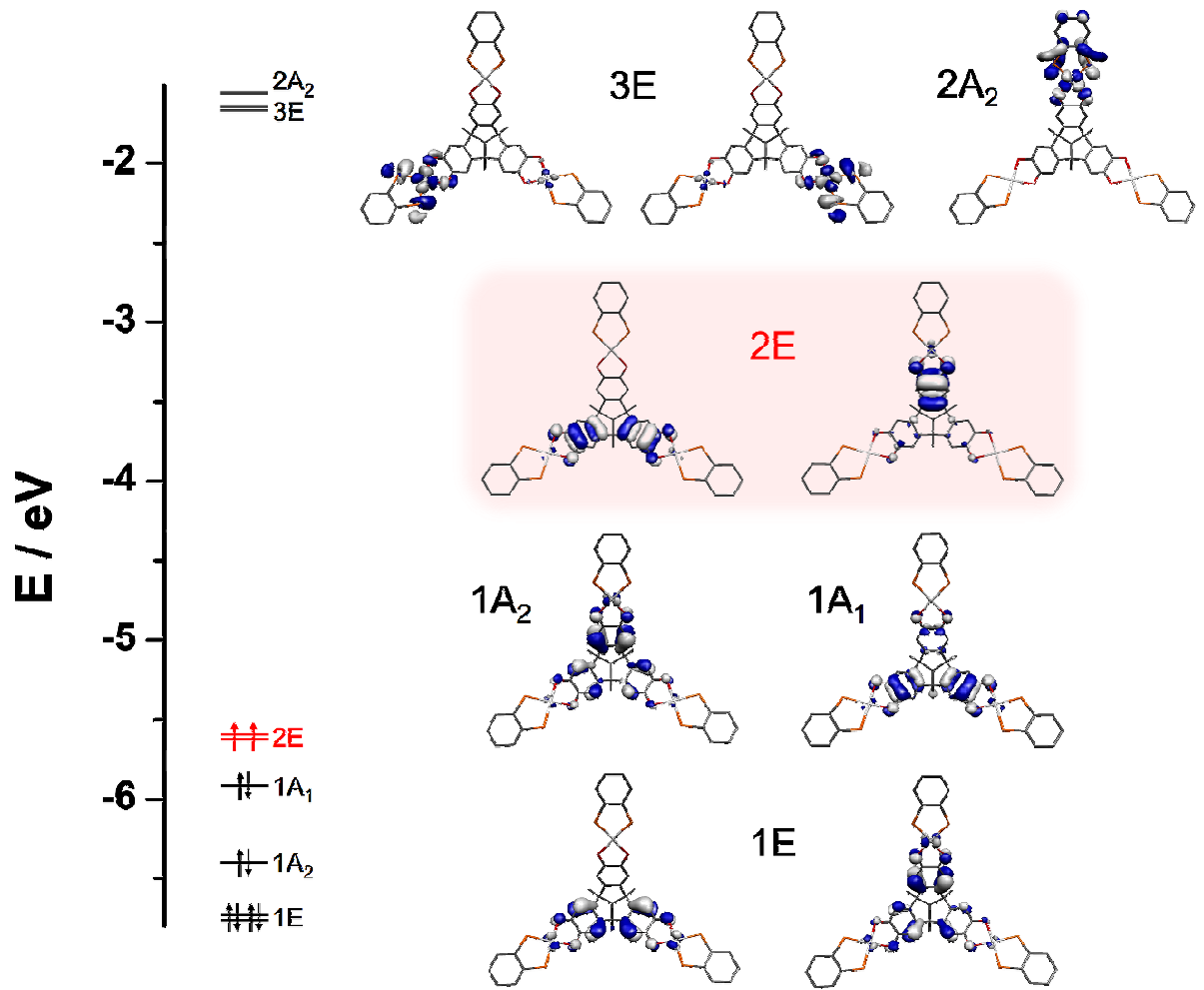


Figure S14. MO energy level scheme of frontier Kohn-Sham orbitals for $[2a^{\bullet\bullet}]^{2+}$ with C_{3v} symmetry labels.

Table S8 Geometry Optimized Coordinates for $[2\text{a}^{\bullet\bullet}]^{3+}$

Pt	5.51173062358761	-3.02067426532468	-0.50639681739674
Pt	0.07837118716684	6.21456878206667	-0.60794029121142
Pt	-5.60027282383056	-2.97320473778080	-0.49118121315418
P	7.63082022867040	-2.47805701982424	-1.03870981887031
P	5.98616183361203	-5.03025517269662	-1.40386113545504
P	-1.43171011341094	7.67636942637959	-1.41501379529211
P	1.62428529345435	7.68624070725527	-1.32405505936560
P	-6.11602750771197	-4.99177757291124	-1.34464773562137
P	-7.70960323410338	-2.40069616352985	-1.03105148855483
O	4.99748380849536	-1.20629580630571	0.37289652951024
O	3.55580361781390	-3.45188788357221	0.06022460066409
O	-1.28383722425413	4.82129862400233	0.12217463656040
O	1.40227079167859	4.82760002306105	0.20052102458112
O	-3.65358753517420	-3.43165341024527	0.08590354381595
O	-5.05030324838209	-1.15177757537403	0.35141751496954
C	1.23984091130018	-1.49588718784134	2.05502287543698
C	2.00068111915222	-0.28632452424441	2.20042658391523
C	3.26325802338416	-0.14958467458996	1.63734078162312
C	3.80179778104672	-1.24009309982819	0.90225135059634
C	3.01372040983642	-2.46925446886299	0.73274192596583
C	1.72288716384889	-2.57058840477233	1.31891484408324
C	-0.03321887044814	-1.46184171537854	2.88902815139955
C	-1.29772326895009	0.76221852461142	3.01921569809484
C	1.26999440362730	0.73931110620038	3.05439514368279
C	0.72511309189006	1.86192669702367	2.17918799439968
C	-0.70929228799011	1.86394174174153	2.14539527069922
C	-1.41674076247114	2.83055355052075	1.44165252505045
C	-0.69157549859902	3.85212997872566	0.77141545951555
C	0.77776110949173	3.85482514453757	0.81299371888926
C	1.46769332281264	2.83217930458627	1.51802460893538
C	-2.04174200044655	-0.25939102785491	2.17329684579473
C	-1.30504229604542	-1.48672798533017	2.05312653261098
C	-1.80755049226312	-2.56474308243580	1.33514007717362
C	-3.09371448452482	-2.44764160409024	0.74154733741742
C	-3.85689558601716	-1.19962691396413	0.88478781206531
C	-3.29887875745366	-0.10703188893952	1.60211663266077
C	8.48370235474264	-3.90264506209822	-1.80425199083363
C	7.72195464414436	-5.08446115549448	-1.97350113635397
C	8.30701618920509	-6.22609678026532	-2.55211533898406
C	9.65040253377937	-6.18055205087334	-2.95851752467353
C	10.40717530200148	-5.00663550504402	-2.79070196760006
C	9.82949532217583	-3.86375674798344	-2.21394398708614
C	-0.59584376209485	9.15800981056594	-2.08380217724172
C	0.81971103149042	9.16301912262070	-2.04081395843345
C	1.53835031226061	10.26822844433851	-2.53306570416455
C	0.83824290517628	11.36322163909278	-3.06512007020429
C	-0.56784979341546	11.35807098244529	-3.10814865339104
C	-1.29114789024381	10.25799166591594	-2.61943870194267
C	-7.85604759179682	-5.02623905084925	-1.90274261042972
C	-8.59420580799604	-3.82644210023458	-1.75725822995035
C	-9.94141720188155	-3.77155029380717	-2.16039672171978
C	-10.54410207650425	-4.91648613519807	-2.70660058578537
C	-9.81079469961426	-6.10826085499479	-2.85071567100159
C	-8.46609828808205	-6.16980888437991	-2.45087586759983
C	-0.03506216152587	-2.67214696671696	3.85548414716758
C	2.20486648511140	1.32498724094628	4.13497785082262
C	-2.23381398517187	1.38943415290014	4.07569108146348
H	7.78207285432921	-1.37864485900651	-1.93718789415092
H	5.17726965590388	-5.41665843806279	-2.51504223845511
H	-2.39234823139915	8.14030047338752	-0.46631282103038
H	2.53537038991244	7.19734582227301	-2.30939807231722
H	-5.32116824143025	-5.41550587172434	-2.45230183828513
H	-7.84238339177797	-1.32120916139953	-1.95641849172006
H	3.87928780393011	0.75106388940786	1.76443762331474
H	1.17393227191251	-3.51568770193967	1.20886057611871
H	-2.51504577653193	2.86362605702741	1.40791003666247

H	2.56626298625661	2.86613728805425	1.54164257113194
H	-1.27872356729663	-3.52336106485347	1.24561625000066
H	-3.89792464244763	0.80714733127570	1.71293218520413
H	7.72456322469902	-7.15049272774742	-2.68771400789639
H	10.11135599776923	-7.07147029744436	-3.40996263188203
H	11.45876583304505	-4.98105454066420	-3.11170107895164
H	10.43117499745713	-2.95074969706560	-2.08507312654516
H	2.63901900240954	10.28356591215721	-2.50249431823057
H	1.39557040870130	12.23071408644510	-3.44870971258245
H	-1.10706186718531	12.22154647091626	-3.52532280267837
H	-2.39167749624684	10.26509224162894	-2.65680048693451
H	-10.52492827144691	-2.84441780438114	-2.05002329260725
H	-11.59693403811502	-4.87836427923977	-3.02221254457301
H	-10.29125652461737	-7.00061576306199	-3.27828124048307
H	-7.90207559182793	-7.10811128566304	-2.56769783223751
H	-0.93438836690146	-2.67401992651250	4.49991318557473
H	0.86472841629456	-2.67618021595757	4.49932868401671
H	-0.03564151036710	-3.61896272713850	3.28129295608369
H	-1.69545594731707	2.12711980456535	4.69998462968017
H	-2.67672130055116	0.61825733529034	4.73382461168143
H	-3.06815539510030	1.92489536971452	3.58191133213658
H	1.67573249083007	2.06682895945356	4.76194745924120
H	3.06145228386223	1.84532811419112	3.66345697414475
H	2.61585007294234	0.53172282239542	4.78709053554071
C	-0.02833329309667	-0.02379641349629	3.59469555669758
C	-0.05084050838414	-0.12921060911606	5.12058359873261
H	-0.04707035082869	0.86431354530723	5.60382500953904
H	0.82820087568519	-0.67981836547615	5.50234036658768
H	-0.95193313326211	-0.66132015159825	5.47677654612723
H	-2.27926539719306	7.18045260498249	-2.45213013311712
H	2.52380933542105	8.15594280323870	-0.31987099773313
H	5.80677463236290	-6.14207206620519	-0.52685457965291
H	8.44094510715529	-2.05754621646143	0.05836058447418
H	-5.95096174163213	-6.08817712042136	-0.44565222647679
H	-8.50599704747633	-1.93637657297586	0.05825615460185

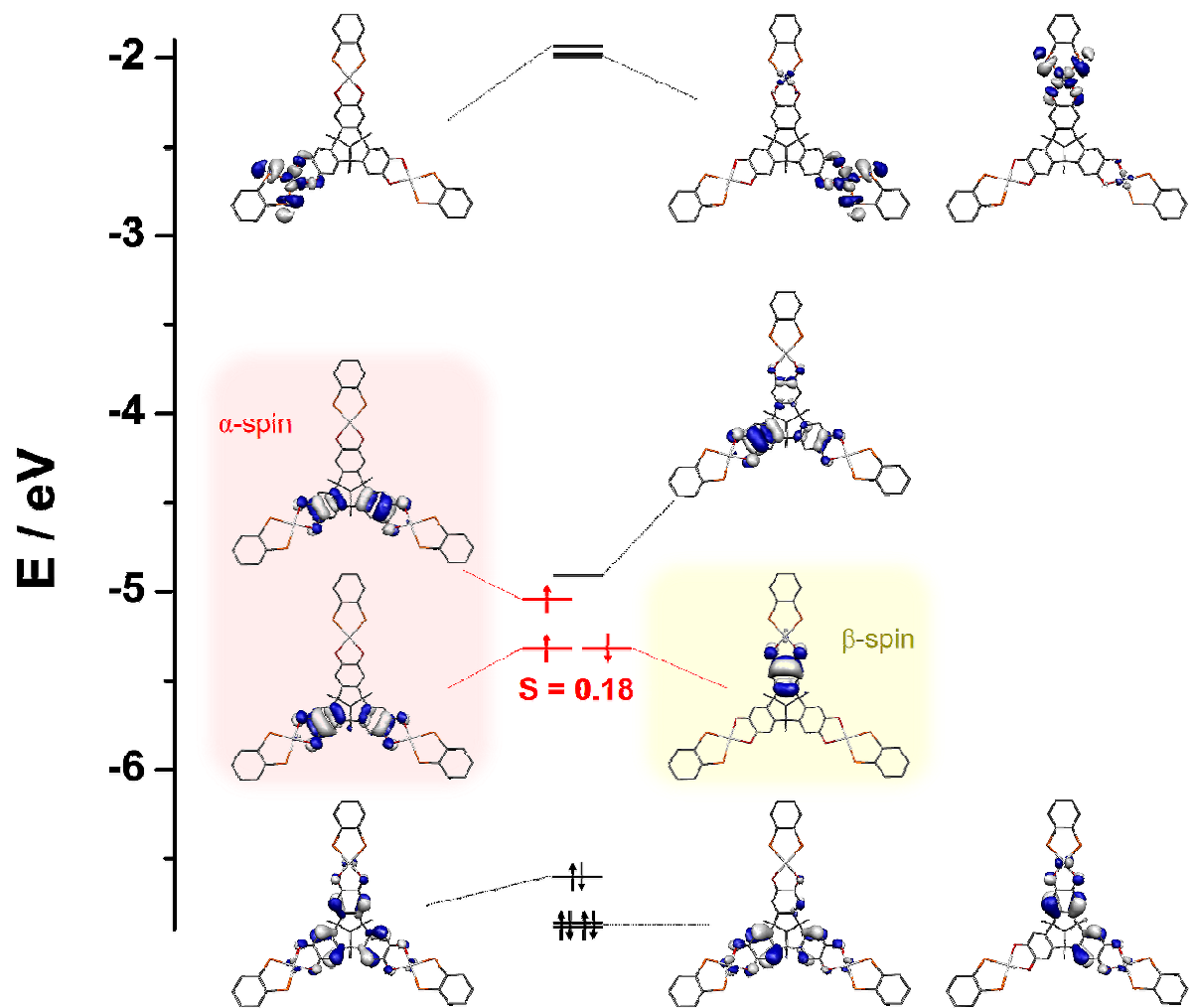


Figure S15. MO energy level scheme of frontier Kohn-Sham orbitals for $[2\mathbf{a}^{\bullet\bullet}]^{3+}$. α -spin and β -spin magnetic orbitals (SOMOs) are highlighted red and yellow, respectively.

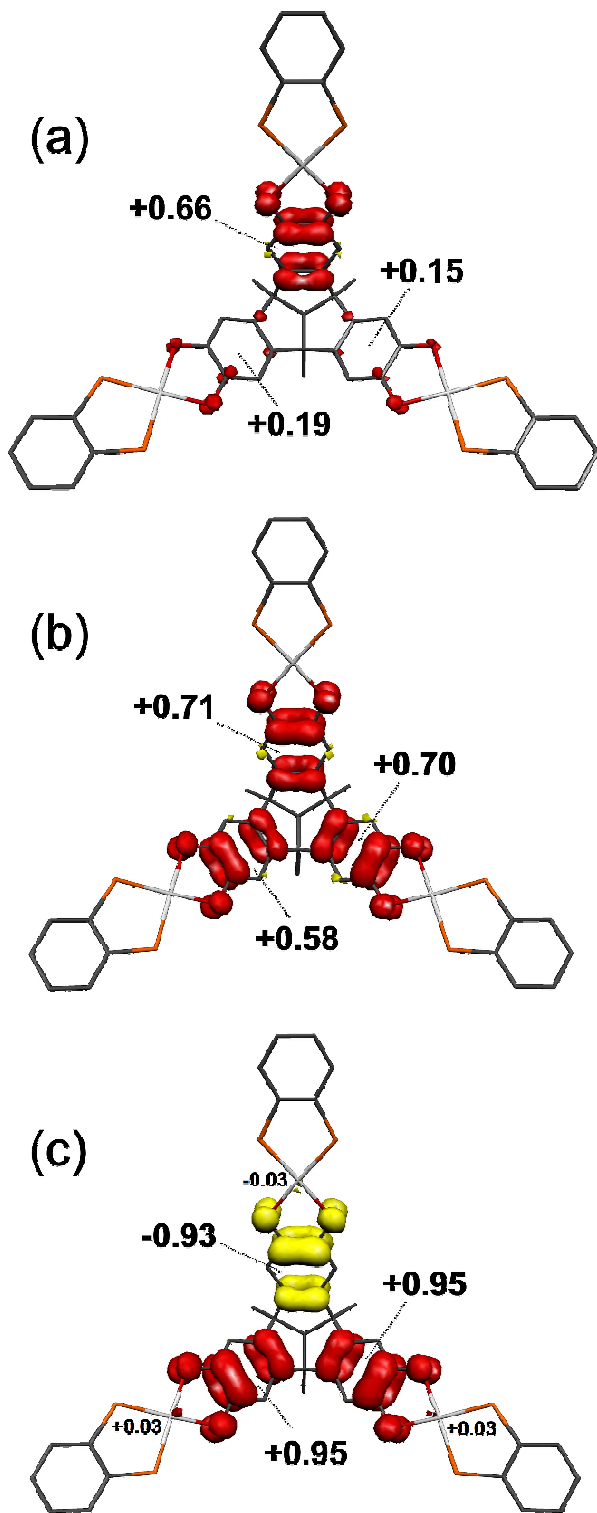


Figure S16. Mulliken spin population analyses for: (a) $[2a^\bullet]^+$, (b) $[2a^{\bullet\bullet}]^+$, and (c) $[2a^{\bullet\bullet\bullet}]^{3+}$ (red: α -spin; yellow: β -spin).

Corresponding data for $[1a^\bullet]^+$, $[1a^{\bullet\bullet}]^+$ and $[1a^{\bullet\bullet\bullet}]^{3+}$ are in Figure 8 of ref. 24.

References

- 1 M. Harig, B. Neumann, H.-G. Stammller and D. Kuck, *Eur. J. Org. Chem.*, 2004, 2381.
- 2 a) W. Levason and C. A. McAuliffe, *Inorg. Chim. Acta*, 1976, **16**, 167;
b) K. Yasufuku, H. Noda and H. Yamazaki, *Inorg. Synth.*, 1989, **26**, 369.
- 3 G. M. Sheldrick, *Acta Crystallogr. Sect. C*, 2015, **71**, 3.
- 4 L. J. Barbour, *J. Supramol. Chem.*, 2001, **1**, 189.
- 5 S. Stoll and A. Schweiger, *J. Magn. Reson.*, 2006, **178**, 42.
- 6 F. Neese, *WIREs Comput. Molec. Sci.*, 2012, **2**, 73.
- 7 a) A. D. Becke, *Phys. Rev. A*, 1988, **38**, 3098;
b) J. P. Perdew, *Phys. Rev. B*, 1986, **33**, 8822.
- 8 S. Grimme, J. Antony, S. Ehrlich and S. Krieg, *J. Chem. Phys.*, 2010, **132**, 154104.
- 9 D. S. Bohle and D. Stasko, *Chem. Commun.*, 1998, 567.
- 10 a) R. Ahlrichs and K. May, *Phys. Chem. Chem. Phys.*, 2000, **2**, 943;
b) F. Weigend and R. Ahlrichs, *Phys. Chem. Chem. Phys.*, 2005, **7**, 3297.
- 11 a) P. Pulay, *Chem. Phys. Lett.*, 1980, **73**, 393;
b) P. Pulay, *J. Comput. Chem.*, 1982, **3**, 556.
- 12 a) A. D. Becke, *J. Chem. Phys.*, 1993, **98**, 5648;
b) C. T. Lee, W. T. Yang and R. G. Parr, *R. G. Phys. Rev. B*, 1988, **37**, 785.
- 13 a) F. Neese, F. Wennmohs, A. Hansen and U. Becker, *Chem. Phys.*, 2009, **356**, 98;
b) R. Izsák and F. Neese, *J. Chem. Phys.*, 2011, **135**, 144105.
- 14 D. A. Pantazis and F. Neese, *J. Chem. Theory Comput.*, 2009, **5**, 2229.
- 15 a) D. A. Pantazis, X.-Y. Chen, C. R. Landis and F. Neese, *J. Chem. Theory Comput.*, 2008, **4**, 908;
b) F. Weigend and R. Ahlrichs, *Phys. Chem. Chem. Phys.*, 2005, **7**, 3297.
- 16 a) E. van Lenthe, J. G. Snijders and E. J. Baerends, *J. Chem. Phys.*, 1996, **105**, 6505;
b) E. van Lenthe, A. van der Avoird and P. E. S. Wormer, *J. Chem. Phys.*, 1998, **108**, 4783;
c) J. H. van Lenthe, S. Faas and J. G. Snijders, *Chem. Phys. Lett.*, 2000, **328**, 107.
- 17 C. J. van Wüllen, *J. Chem. Phys.*, 1998, **109**, 392.
- 18 A. V. Marenich, C. J. Cramer and D. G. Truhlar, *J. Phys. Chem. B*, 2009, **113**, 6378.
- 19 a) L. Noodleman, *J. Chem. Phys.*, 1981, **74**, 5737;
b) L. Noodleman, D. A. Case and A. Aizman, *J. Am. Chem. Soc.*, 1988, **110**, 1001;
c) L. Noodleman and E. R. Davidson, *Chem. Phys.* **1986**, **109**, 131;
d) L. Noodleman, J. G. Norman, J. H. Osborne, A. Aizman and D. A. Case, *J. Am. Chem. Soc.*, 1985, **107**, 3418;
e) L. Noodleman, C. Y. Peng, D. A. Case and J. M. Monesca, *Coord. Chem. Rev.*, 1995, **144**, 199.
- 20 F. Neese, *J. Phys. Chem. Solids*, 2004, **65**, 781.
- 21 *Molekel*, Advanced Interactive 3D-Graphics for Molecular Sciences, Swiss National Supercomputing Center.
<https://ugovaretto.github.io/molekel/>
- 22 a) J. A. Hyatt, E. N. Duesler, D. Y. Curtin and I. C. Paul, *J. Org. Chem.*, 1980, **45**, 5074;
b) A. Chakrabarti, H. M. Chawla, G. Hundal and N. Pant, *Tetrahedron*, 2005, **61**, 12323;
c) C. J. Sumby and M. J. Hardie, *Acta Cryst. Sect. E*, 2007, **63**, o1537.
- 23 J. J. Loughrey, C. A. Kilner, M. J. Hardie and M. A. Halcrow, *Supramol. Chem.*, 2012, **24**, 2.
- 24 J. J. Loughrey, N. J. Patmore, A. Baldansuren, A. J. Fielding, E. J. L. McInnes, M. J. Hardie, S. Sproules and M. A. Halcrow, *Chem. Sci.*, 2015, **6**, 6935.
- 25 Y. S. Sohn, D. N. Hendrickson and H. B. Gray, *J. Am. Chem. Soc.*, 1970, **92**, 3233.

- 26 a) J. A. Weinstein, M. T. Tierney, E. S. Davies, K. Base, A. A. Robeiro and M. W. Grinstaff, *Inorg. Chem.*, 2006, **45**, 4544;
b) J. Best, I. V. Sazanovich, H. Adams, R. D. Bennett, E. S. Davies, A. J. H. M. Meijer, M. Towrie,
S. A. Tikhomirov, O. V. Bouganov, M. D. Ward and J. A. Weinstein, *Inorg. Chem.*, 2010, **49**, 10041;
c) J. J. Loughrey, S. Sproules, E. J. L. McInnes, M. J. Hardie and M. A. Halcrow, *Chem. Eur. J.*, 2014, **20**,
6272.